RCP-Bench: Benchmarking Robustness for Collaborative Perception Under Diverse Corruptions

Supplementary Material

This technical appendix provides supplementary details regarding the proposed RCP-Bench, along with experimental results that were excluded from the main body of this paper due to page limitations.

Specifically, this appendix is organized as follows:

- Sec. A presents detailed definitions of our sensor corruption types.
- Sec. B provides comprehensive definitions of typical corruption cases within RCP-Bench.
- Sec. C presents additional results related to the OPV2V-C benchmark.
- Sec. D offers more experimental results and additional ablation studies for RCP-Drop and RCP-Mix.
- Sec. E presents further results on V2XSet-C.
- Sec. F includes additional results on DAIR-V2X-C.
- Sec. G presents further segmentation results on OPV2V-C.
- Sec. H includes qualitative results for the benchmarked methods under each corruption type.

A. Definition and Analysis of Sensor Corruption

Real-world corruptions can arise from multiple and diverse sources. For instance, an autonomous vehicle may simultaneously encounter adverse weather conditions and unusual objects, resulting in significantly more complex corruptions. While it is impossible to enumerate all potential real-world corruptions, we systematically design 14 corruption types categorized into five levels, which serve as a practical testbed for conducting controlled robustness evaluations. In this section, we provide detailed descriptions and configurations of the camera sensor corruptions utilized in our RCP-Bench. These corruptions are intended to simulate various real-world conditions that autonomous driving systems may face. The specific types of corruptions are as follows:

- **Bright** and **Dark**: These conditions simulate various lighting environments to evaluate the robustness of collaborative perception methods across different illumination scenarios.
- **Fog**, **Frost**, and **Snow**: These represent visually obstructive forms of precipitation, simulating extreme weather conditions that can obscure the camera's view.
- **Quant**: This technique reduces the number of colors in an image while maintaining its overall visual integrity, thereby challenging the model's capacity to manage color variations.

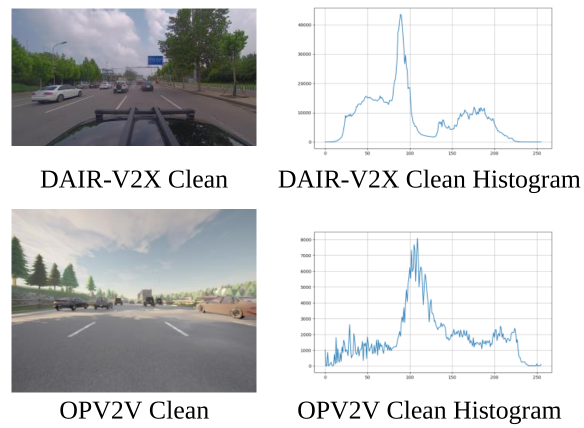

Figure 1. Visualizations of clean camera and histogram on DAIR-V2X and OPV2V

- **Camera Crash**: This simulates the continuous loss of images from specific viewpoints due to camera malfunction.
- **Blur**: Images captured by the camera may lack clarity and exhibit blurriness. This paper primarily addresses three types of blur: Zoom Blur, Motion Blur, and Defocus Blur. Defocus blur occurs when an image is out of focus, motion blur arises when the camera moves rapidly, and zoom blur is observed when the camera quickly approaches an object.
- **Noise**: Captured images may be affected by noise disturbances. This study examines three types of noise: Gaussian noise, Impulse noise, and Shot noise. Gaussian noise is typically present in low-light conditions, shot noise (also known as Poisson noise) results from the discrete nature of light, and impulse noise is a color analogue of salt-and-pepper noise, which can occur due to bit errors.
- **Temporal Misalignment**:Variations in camera configurations among collaborative vehicles, differing camera frequencies, and misaligned clocks can result in non-simultaneous capture of shared information, thereby diminishing collaborative effectiveness. Due to limitations in the dataset's time frames, generating images at arbitrary time points is not feasible; therefore, in these simulations, we randomly adjust the time frames of surrounding shared vehicles either forward or backward based on the degree of disturbance.

We selected the real-world dataset DAIR-V2X and the simulated dataset OPV2V as representatives for our analysis. Visualization examples of camera sensor corruptions

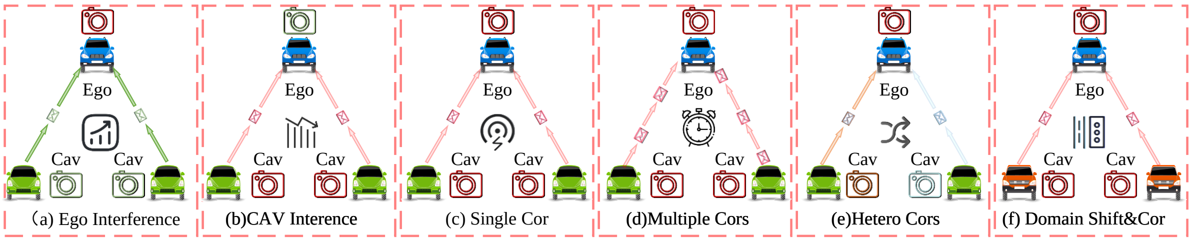

Figure 2. Definitions of evaluation scenarios in RCP-Bench.

at varying severity levels are presented in Table 3 and Fig 4. We calculated the pixel distribution sampled from the OPV2V-C and DAIR-V2X-C datasets and visualized the pixel histograms, as shown in Fig 5 and 6. Notably, the experimental results in the manuscript indicate that Gaussian, Impulse, and Shot noise types led to the least shifts in pixel distribution, although they caused a relatively significant drop in performance. In contrast, Snow noise caused a noticeable shift in pixel distribution toward lower values, and color quantization rendered fine-grained features less distinct by shifting pixel values more aggregately. However, these two types of corruption only resulted in the smallest performance gaps. This suggests that model robustness is not solely correlated with pixel distribution.

Regarding the specific perturbation settings, we implemented 14 types of perturbations on OPV2V and V2XSet. However, since both the vehicle and road sides of DAIR-V2X utilize only a single camera, the occurrence of the ”Camera Crash” corruption results in complete failure on one side. Consequently, we only considered 13 types of perturbations in DAIR-V2X.

B. Definition of Typical Corruption Cases in RCP-Bench

RCP-Bench is designed to systematically evaluate three collaborative scenarios across six cases: assessing robustness in the Global Interference scenario, exploring collaborative advantages in the Ego Interference scenario (see Fig 2 (a)), and examining disturbance risks in the CAV Interference scenario (see Fig 2 (b)). Consequently, we differentiate only between the ego vehicle and the surrounding collaborative vehicles, assuming that all collaborative vehicles maintain consistent states. In addition to the scenarios where the ego vehicle and collaborative vehicles experience consistent disturbances, as detailed in Fig 2 (c), we will elaborate on three more complex scene setups within the Global Interference scenario.

Multiple Corruptions: In real collaborative processes, multiple disturbance situations may occur simultaneously. However, generating a dataset that accurately reflects these various disturbances is challenging. Therefore, when considering overlay disturbances, we focus on a more plausible and easily implementable scenario: the misalignment of collaborative timing combined with 13 other disturbance methods. The schematic representation is shown in Fig 2 (d). Specific experimental results can be found in Fig 7.

Heterogeneous Corruptions, : In collaborative processes, the types of disturbances experienced by different collaborative vehicles are often inconsistent. To simulate this mixed disturbance situation, we considered three independently occurring disturbance types: Dark, Motion Blur, and Camera Crash. The schematic representation is shown in Fig 2 (e). Specific experimental results can be found in Fig 8.

New Scenes with Corruption: The introduction of the Culver dataset emphasizes that the generalization of collaboration has always been a focal point of research, including various weather scenarios [2–4] and migration from Sim2Real [5]. The Culver dataset is specifically designed to evaluate collaboration in new traffic scenarios under OPV2V settings. To assess the generalization capability of the collaborative model, we tested the model trained on OPV2V using the Culver dataset. Additionally, we generated a disturbance dataset for Culver to increase the difficulty of simulating model performance in unknown new scenarios where the camera experiences disturbances. Specifically, we considered 14 types of disturbances.

C. Additional Results on OPV2V-C

The complete results concerning the Relative Corruption Error (CE), along with additional findings for Multiple Corruptions and Hetero Corruptions, are presented in Table 6, Figure 7, and Figure 8, respectively. Furthermore, the results for Global Interference at AP@0.3 and AP@0.7 are provided in Table 5, Table 7, Table 8, and Table 9. The results for Ego Interference and CAV Interference are displayed in Table 10 and Table 11.

D. More results of RCP-Drop&RCP-Mix

Ablation study of RCP-Drop: Additional ablation studies of AttFuse [12] on OPV2V-C are presented in Table 1. We compare the performance of using different fixed dropout probabilities with our dynamic adjustment strategy. Specifically, when dropout = 0, it represents the baseline model, which utilizes all the information from the collaborators. It is evident that our dynamic adjustment strategy significantly outperforms the fixed threshold approaches.

Table 1. Ablation study of RCP-Drop

Dropout	0	0.1	0.3	0.5	0.7	0.9	RCP-Drop
$\mathrm{AP}_{clean}\uparrow$	37.13	40.25	42.68	38.18	39.66	40.44	**45.18**
$\mathrm{mAP}_{cor}\uparrow$	15.99	24.83	25.92	23.80	22.74	22.49	**27.56**
$\mathrm{mNegC}\downarrow$	121.59	122.78	119.83	117.8	125.63	121.74	**115.64**
$\mathrm{mPosC}\uparrow$	16.97	19.85	**20.94**	19.42	17.45	10.19	18.17

Ablation study of RCP-Mix: Our RCP-Mix method is inspired by Mixstyle [13, 14]. However, Mixstyle [13, 14] focuses on the overall collaborative scenario, whereas RCP-Mix emphasizes individual CAVs within the same scenario. Given the varying numbers of CAVs across different scenarios, we applied the Mixstyle operation to the integrated features. To enhance the effectiveness of Mixstyle, we adjusted the RCP-Bench batch size from 1 to 4. The experimental results are shown in Table 2. It can be observed that both Mixstyle and RCP-Mix improve the model performance, with RCP-Mix achieving a greater improvement than Mixstyle. Moreover, since they operate from different dimensions, they can be combined. Our experiments revealed that simultaneous mixing at both levels further enhances robust performance.

Table 2. Ablation study of RCP-Mix

batchsize=4	$\mathrm{AP}_{clean}\uparrow$	$\mathrm{mAP}_{cor}\uparrow$	$\mathrm{mNegC}\downarrow$	$\mathrm{mPosC}\uparrow$
AttFuse [12]	48.13	29.75	113.16	19.6
+Mixstyle [4]	50.51	31.94	108.54	21.81
+RCP-Mix	49.67	33.16	110.06	23.14
+Mixstyle+RCP-Mix	**52.17**	**34.33**	**105.63**	**24.46**

Experiments with model adaptation techniques: in the manuscript, we incorporate online Batch Normalization (BN) Adapt as a baseline to assess the effectiveness of methods developed for single-vehicle perception. We further evaluate Tent [8], a classical test-time adaptation algorithm. The results on OPV2V-C (Table 4 in the manuscript and the following table) indicate that while BN and Tent improve robustness under individual perturbations, they fail to jointly mitigate mNegC and may even degrade clean performance. In contrast, our RCP-Mix and RCP-Drop, specifically designed for collaborative perturbations, significantly enhance robustness, emphasizing the necessity of dedicated methods to improve the robustness of collaborative perception.

Table 3. Comparison with model adaptation techniques

	$\mathrm{AP}_{clean}\uparrow$	$\mathrm{mAP}_{cor}\uparrow$	$\mathrm{mNegC}\downarrow$	$\mathrm{mPosC}\uparrow$
AttFuse [12]	37.13	15.99	121.59	16.97
+Tent [6]	36.45	21.75	125.12	19.29
+Tent+RCP-Mix	**45.76**	25.61	115.27	18.61
+Tent+RCP-Drop	43.28	**27.59**	**114.67**	**22.58**

Ablation study of RCP-Drop&RCP-Mix: The experimental results in the manuscript demonstrate that, despite the relative simplicity of the RCP-Drop and RCP-Mix methods, they effectively mitigate performance degradation caused by data corruption. We further examined whether the combination of these two proposed methods would yield superior results in Table 4. The findings indicate that their combined effect can enhance training outcomes on the original clean training set, denoted as AP_{clean}. However, AP_{cor}, mNegC, and mPosC cannot be solely attributed to either RCP-Drop or RCP-Mix. We contend that the model's optimization on the clean training set is overly idealized, which may lead to suboptimal performance when faced with new perturbation scenarios. Table 12,Table 13 and Table 14 presents detailed experimental results for CoBEVT [10] and its variants, including mAP_{cor}, mNegC, and mPosC. Additionally, Table 15, Table 16 and Table 17 displays comprehensive experimental results for AttFuse and its variants, encompassing mAP_{cor}, mNegC, and mPosC.

Table 4. Efficacy of RCP-Drop and RCP-Mix on collaborative robustness, collaborative compensation and collaborative disruption.

	$\mathrm{AP}_{clean}\uparrow$	$\mathrm{mAP}_{cor}\uparrow$	$\mathrm{mNegC}\downarrow$	$\mathrm{mPosC}\uparrow$
CoBEVT [10]	40.49	15.91	111.48	14.29
+BN [7]	42.74	27.87	112.94	18.28
+BN+RCP-Mix	48.25	31.83	**109.11**	**23.44**
+BN+RCP-Drop	47.84	30.68	109.45	20.07
+BN+RCP-Drop+RCP-Mix	**54.49**	**32.55**	109.23	23.04
AttFuse [12]	37.13	15.99	121.59	16.97
+BN [7]	36.13	22.35	126.04	18.85
+BN+RCP-Mix	43.12	**28.85**	**114.97**	**22.51**
+BN+RCP-Drop	45.18	27.56	115.64	18.17
+BN+RCP-Drop+RCP-Mix	**49.34**	26.84	117.59	17.21

E. Additional Results on V2XSet-C

We conducted three significant validation experiments on V2XSet-C, focusing on the collaborative robustness metric AP_{cor} under the Global Interference scenario at thresholds of AP@0.3, AP@0.5, and AP@0.7, as detailed in Table 21, Table 19, and Table 23; and Table 20, Table 18, and Table 22. Additionally, the metrics for collaborative compensation (mPosC) and collaborative disruption (mNegC) under the Ego Interference and Cav Interference scenarios at AP@0.3, AP@0.5, and AP@0.7 are presented in Table 24, Table 25, and Table 26.

F. Additional Results on DAIR-V2X-C

Given that DAIR-V2X-C comprises only two cooperative devices—one on the vehicle side and one on the road side—each equipped with a single camera, the performance at AP@0.7 is suboptimal. Consequently, we focus solely on the metrics for AP@0.3 and AP@0.5, which include the experimental results for collaborative robustness (AP_{cor}) and RCE under the Global Interference scenario, as presented in Tables 30, 28, 29, and 27. Additionally, in both the Ego Interference scenario and the Cav Interference scenario, the metrics for collaborative compensation (mPosC) and collaborative disruption (mNegC) are detailed in Tables 31 and 32.

G. Additional Segmentation Results on OPV2V-C

Leveraging the additional semantic information provided by OPV2V, we undertook a preliminary investigation of the collaborative semantic segmentation task. The test scenarios were designed based on the collaborative detection framework, while preserving the computational metrics relevant to semantic segmentation. The experimental results, presented in Tables 33 and 34, demonstrate that existing semantic segmentation models display limited robustness when faced with disturbances caused by collaborative vehicles.

H. Visualization Results

We present additional visualization results for detection and segmentation of the OPV2V-C, as illustrated in Fig 9.

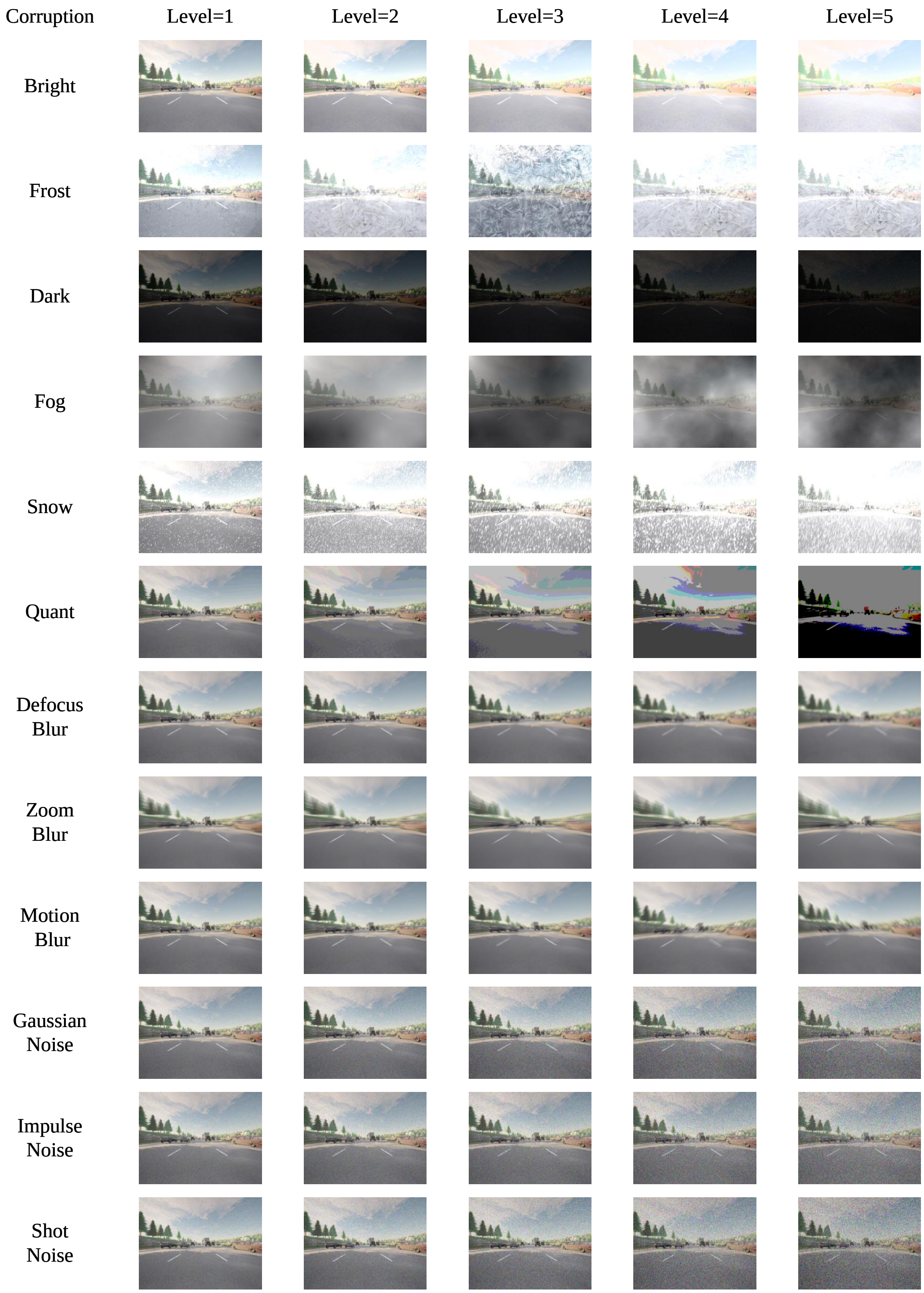

Figure 3. Visualizations of different Camera sensor corruptions on OPV2V-C under 5 severity levels

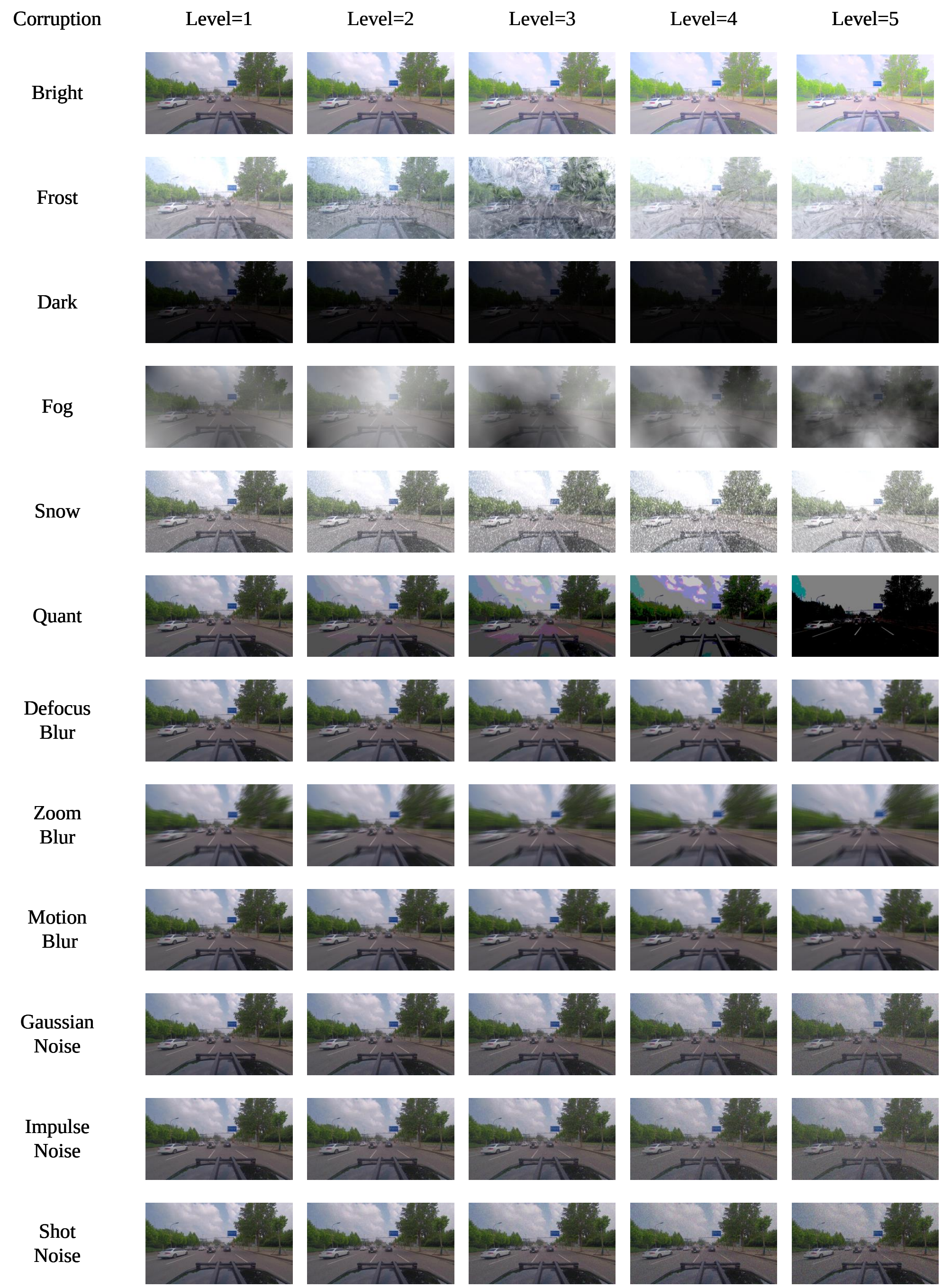

Figure 4. Visualizations of different Camera sensor corruptions on DAIR-V2X-C under 5 severity levels

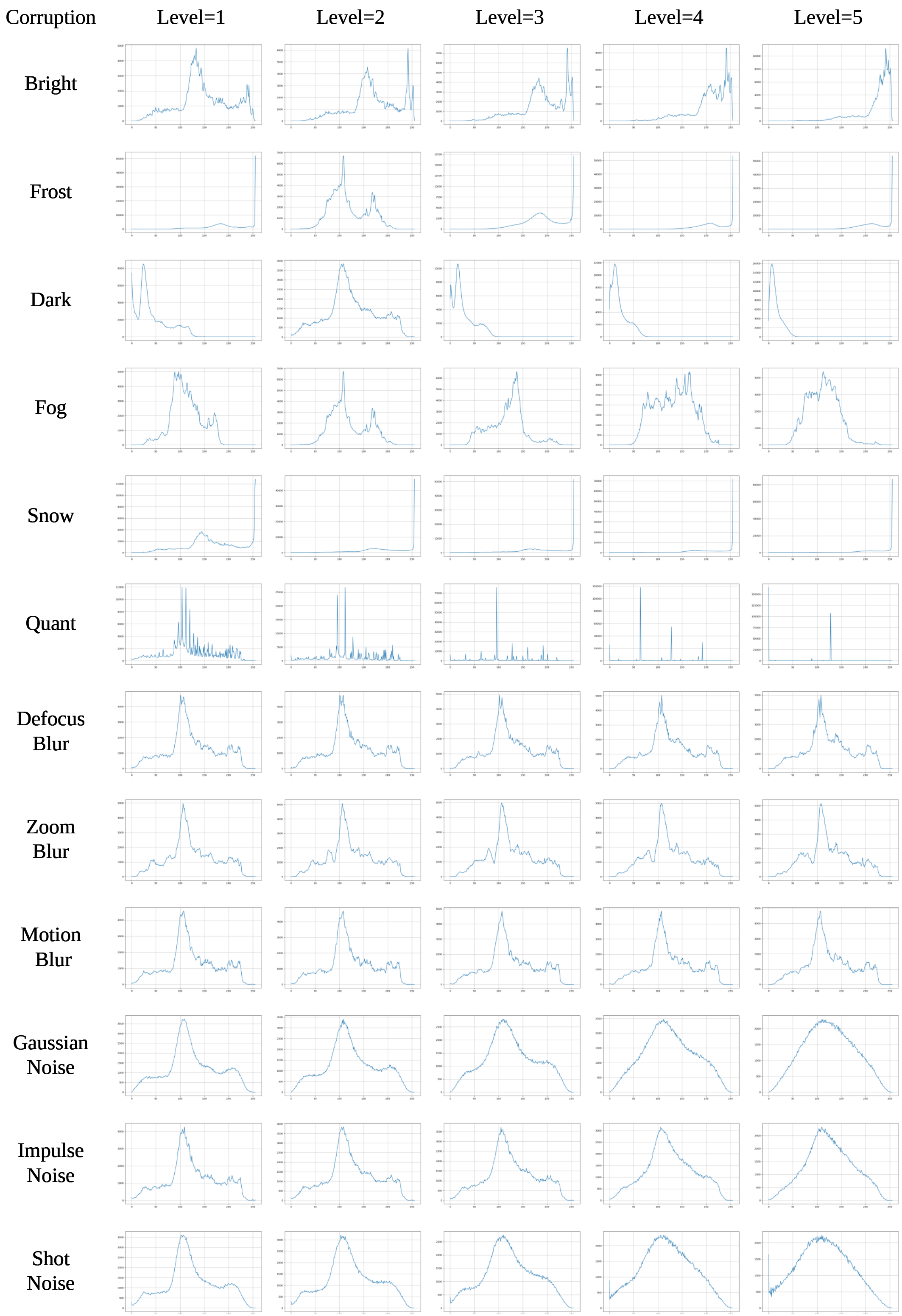

Figure 5. The pixel histogram of each corruption type in the OPV2V-C under 5 severity levels

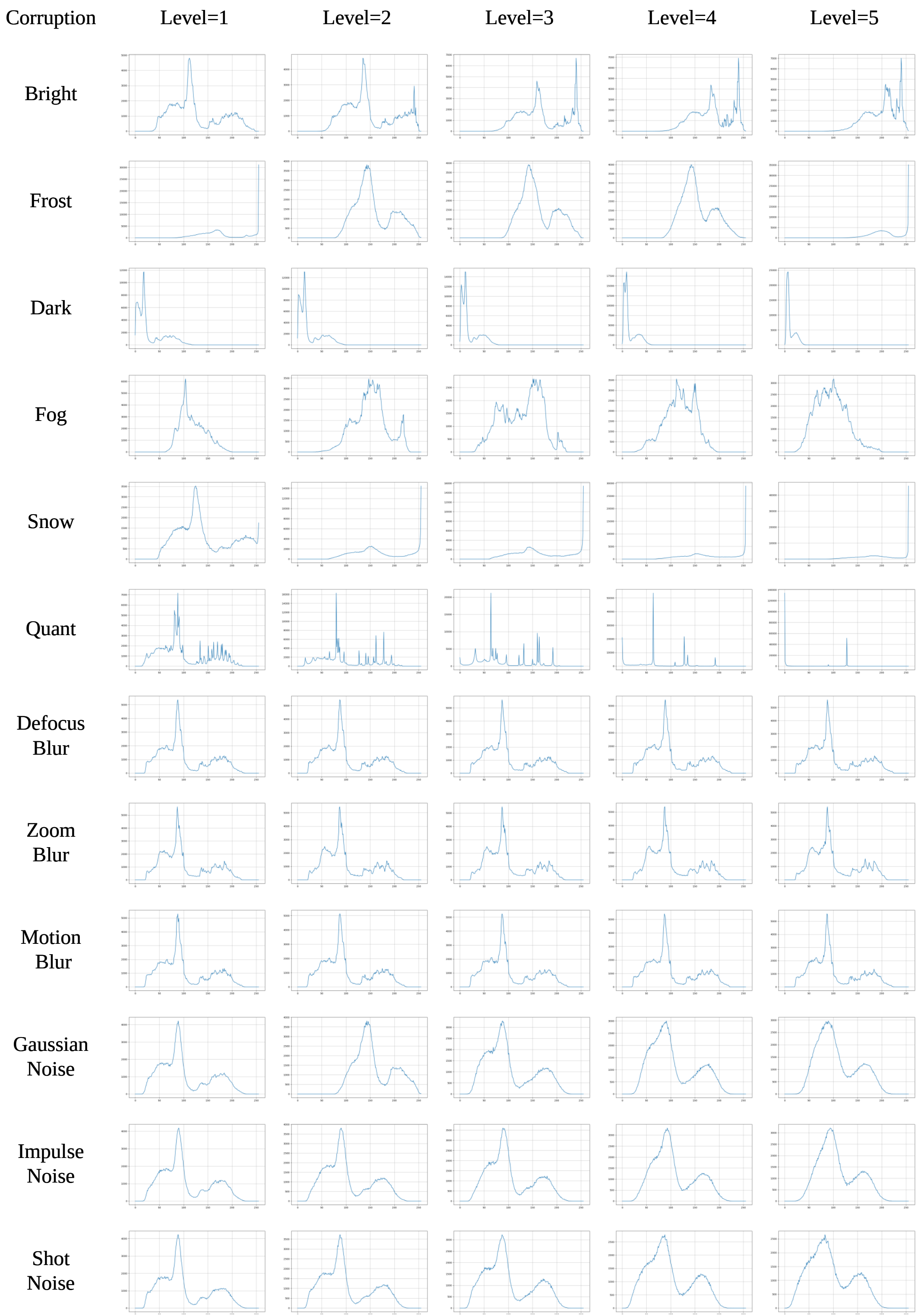

Figure 6. The pixel histogram of each corruption type in the DAIR-V2X-C under 5 severity levels

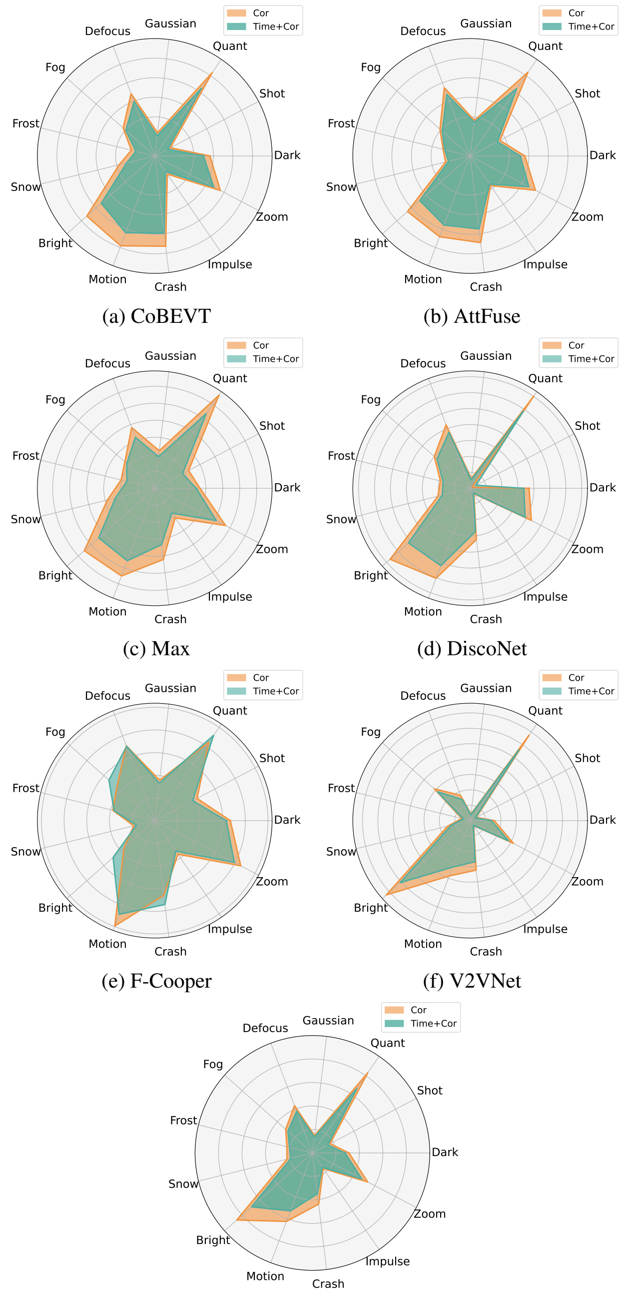

(a) CoBEVT (b) AttFuse (c) Max (d) DiscoNet (e) F-Cooper (f) V2VNet (g) V2X-ViT

Figure 7. Radar charts for CoBEVT [10] ,AttFuse [12], Max, DiscoNet [6], F-Cooper [1], V2VNet [9] and V2X-ViT [11] showing performance under single corruptions (labeled as "Cor" in the figure) and multiple corruptions that include additional temporal misalignment (labeled as "Time" in the figure).

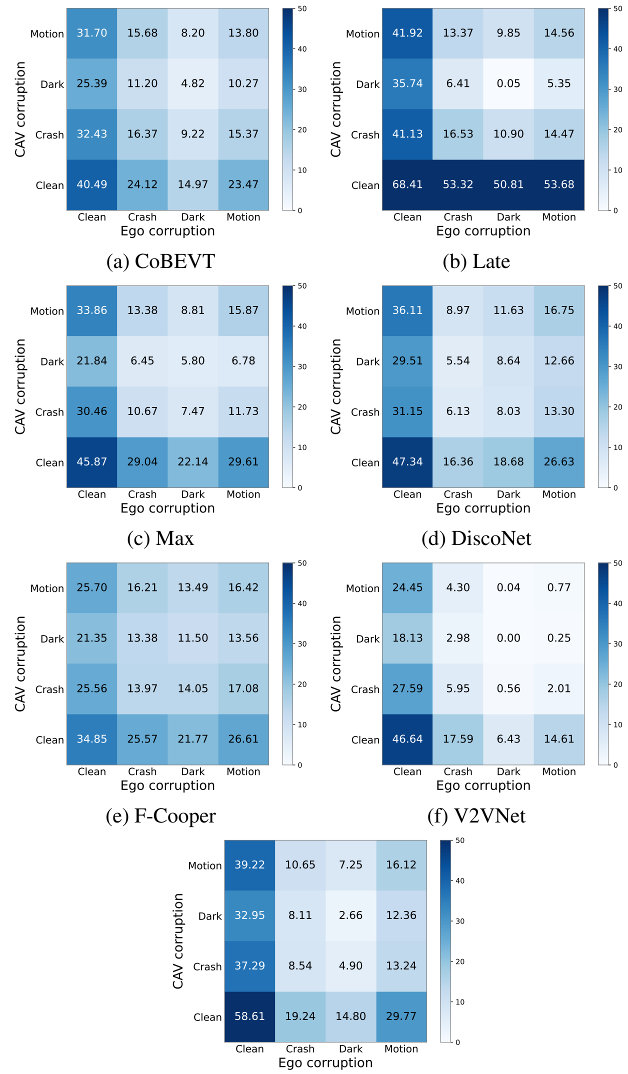

(a) CoBEVT (b) Late (c) Max (d) DiscoNet (e) F-Cooper (f) V2VNet (g) V2X-ViT

Figure 8. Results of CoBEVT [10], Late, Max, V2VNet [9] and DiscoNet [6], F-Cooper [1] and V2X-ViT [11] in terms of AP_{cor} under heterogeneous corruptions between Ego and CAVs.

Figure 9. Qualitative comparison of each type of corruption on OPV2V-C. The green and red 3D bounding boxes represent the ground truth and predictions, respectively.

Table 5. Benchmarking results for Global Interference on OPV2V-C. We report the performance under each corruption RCE and the overall corruption robustness mRCE averaged over all corruption types. The results are evaluated based on AP@0.3.

Cortype	AttFuse [12]	F-Cooper [1]	V2X-ViT [11]	DiscoNet [6]	V2VNet [9]	CoBEVT [10]	Max	Late	NoFusion
$\mathrm{AP}_{clean}\uparrow$	56.63	51.42	73.16	64.89	68.74	64.87	67.06	82.57	49.38
Bright	38.77	68.39	20.29	25.00	19.32	35.70	38.06	24.33	24.59
Dark	67.28	58.57	67.82	63.45	78.88	66.30	71.69	67.80	73.13
Fog	78.23	72.80	73.37	72.66	65.85	77.56	77.75	81.01	83.24
Frost	83.32	76.09	76.86	79.16	91.71	80.57	77.72	83.83	84.84
Snow	81.79	84.97	74.86	74.64	77.56	71.54	68.70	81.91	82.20
Gaussian	79.22	74.85	83.56	90.30	93.89	82.68	74.95	79.82	82.85
Impulse	79.60	75.26	82.27	92.69	94.19	83.31	75.81	78.20	81.88
Shot	80.18	71.52	81.21	91.26	92.94	85.93	74.44	77.19	80.62
Zoom	53.96	43.42	49.33	53.43	56.67	54.81	47.04	54.54	62.25
Motion	45.94	36.07	42.50	40.74	53.05	43.71	41.00	40.77	52.53
Defocus	57.42	57.52	61.50	59.97	77.45	62.07	60.42	75.04	82.44
Crash	41.97	50.93	53.47	61.94	58.43	40.77	52.97	53.19	62.11
Quant	30.35	35.99	24.33	24.76	23.57	31.67	26.45	29.64	32.76
Tempormis	14.41	26.47	12.32	13.06	10.41	14.39	13.80	15.56	0.00
$\mathrm{mRCE}\downarrow$	59.46	59.49	57.41	60.22	63.85	59.36	57.20	60.20	63.25

Table 6. Benchmarking results for Global Interference on OPV2V-C. We report the performance under each corruption RCE and the overall corruption robustness mRCE averaged over all corruption types. The results are evaluated based on AP@0.5.

Cortype	AttFuse [12]	F-Cooper [1]	V2X-ViT [11]	DiscoNet [6]	V2VNet [9]	CoBEVT [10]	Max	Late	NoFusion
$\mathrm{AP}_{clean}\uparrow$	37.13	34.85	58.61	47.34	46.64	40.49	45.87	68.41	35.68
Bright	42.38	74.04	26.53	29.13	21.90	42.76	39.70	24.33	29.31
Dark	62.28	52.11	73.42	60.96	83.18	65.14	70.94	67.80	74.94
Fog	72.26	68.01	74.01	68.28	66.60	73.38	74.42	81.01	87.46
Frost	80.83	72.62	80.87	79.67	93.95	84.84	77.79	83.83	88.20
Snow	82.60	86.32	80.90	77.99	83.82	76.87	68.76	81.91	86.69
Gaussian	75.30	74.23	87.30	93.44	95.40	85.25	75.74	79.82	85.35
Impulse	75.31	74.16	86.17	95.61	95.64	86.06	76.97	78.20	84.45
Shot	76.89	69.72	85.53	98.50	95.12	88.86	75.46	77.19	82.52
Zoom	49.22	38.47	54.66	54.21	65.93	53.20	48.72	54.54	63.86
Motion	40.57	28.63	46.78	36.28	58.74	39.36	39.91	40.77	51.75
Defocus	49.79	49.35	63.20	55.07	81.14	57.99	58.39	75.04	81.64
Crash	39.94	52.30	62.53	65.75	65.29	42.64	54.05	53.19	61.86
Quant	29.95	39.64	29.22	25.87	27.78	36.14	27.46	29.64	33.86
Tempormis	19.91	19.51	18.25	16.95	16.93	17.57	19.66	27.97	0.00
$\mathrm{mRCE}\downarrow$	56.95	57.08	62.10	61.27	67.96	60.72	57.71	61.09	65.13

Table 7. Benchmarking results for Global Interference on OPV2V-C. We report the performance under each corruption RCE and the overall corruption robustness mRCE averaged over all corruption types. The results are evaluated based on AP@0.7.

Cortype	AttFuse [12]	F-Cooper [1]	V2X-ViT [11]	DiscoNet [6]	V2VNet [9]	CoBEVT [10]	Max	Late	NoFusion
$\mathrm{AP}_{clean}\uparrow$	12.90	11.52	31.41	19.56	12.18	12.11	16.02	43.02	17.16
Bright	37.80	74.97	37.41	27.07	20.64	54.91	38.36	34.15	38.43
Dark	43.57	17.38	71.55	48.24	83.19	55.09	66.10	75.81	78.33
Fog	47.53	39.62	78.29	49.46	57.27	58.65	62.52	91.06	94.08
Frost	65.41	53.26	83.16	71.51	95.53	89.68	71.07	91.02	92.56
Snow	77.07	81.02	88.39	80.13	87.50	83.98	61.17	89.57	90.66
Gaussian	66.60	62.64	87.06	96.48	94.37	83.12	71.09	88.14	89.57
Impulse	62.98	59.97	86.58	98.08	95.14	85.52	71.61	87.11	88.88
Shot	71.49	53.63	85.97	97.88	94.96	89.83	70.67	85.28	85.83
Zoom	37.98	14.83	61.98	47.45	80.38	38.33	46.44	72.70	75.64
Motion	21.44	-3.04	50.65	23.81	58.28	27.18	36.69	50.19	56.41
Defocus	17.98	15.05	63.74	38.68	83.96	41.87	53.46	81.73	84.16
Crash	31.05	41.61	70.95	65.61	49.93	35.11	51.84	57.74	62.38
Quant	31.47	38.70	38.56	21.33	31.54	40.71	26.64	34.91	36.22
Tempormis	21.38	21.37	21.80	19.61	26.24	15.69	23.26	45.76	0.00
$\mathrm{mRCE}\downarrow$	45.27	40.79	66.15	56.10	68.50	57.12	53.64	70.37	69.51

Table 8. Benchmarking results for Global Interference on OPV2V-C. We report the performance under each corruption AP_c and the overall corruption robustness AP_{cor} averaged over all corruption types. The results are evaluated based on AP@0.3.

Cortype	AttFuse [12]	F-Cooper [1]	V2X-ViT [11]	DiscoNet [6]	V2VNet [9]	CoBEVT [10]	Max	Late	NoFusion
$\mathrm{AP}_{clean}\uparrow$	56.63	51.42	73.16	64.89	68.74	64.87	67.06	82.57	49.38
Bright	34.67	16.25	58.32	48.67	55.46	41.71	41.53	51.76	37.24
Dark	18.53	21.30	23.54	23.72	14.52	21.86	18.99	22.03	13.27
Fog	12.33	13.99	19.48	17.74	23.48	14.56	14.92	12.99	8.28
Frost	9.44	12.29	16.93	13.52	5.70	12.60	14.94	11.06	7.49
Snow	10.31	7.73	18.40	16.45	15.43	18.46	20.99	12.37	8.79
Gaussian	11.77	12.93	12.03	6.30	4.20	11.24	16.80	13.80	8.47
Impulse	11.55	12.72	12.97	4.74	3.99	10.83	16.22	14.91	8.95
Shot	11.22	14.64	13.75	5.67	4.85	9.13	17.14	15.60	9.57
Zoom	26.07	29.10	37.07	30.22	29.78	29.32	35.52	31.10	18.64
Motion	30.61	32.87	42.07	38.46	32.28	36.51	39.57	40.52	23.44
Defocus	24.11	21.84	28.17	25.97	15.50	24.60	26.54	17.07	8.67
Crash	32.86	25.23	34.04	24.69	28.58	38.42	31.54	32.02	18.71
Quant	39.44	32.92	55.36	48.83	52.54	44.32	49.32	48.13	33.20
Tempormis	48.47	43.81	64.14	56.42	61.58	55.54	57.81	69.73	49.39
$\mathrm{AP}_{cor}\uparrow$	22.96	21.26	31.16	25.81	24.85	26.37	28.70	28.08	18.15

Table 9. Benchmarking results for Global Interference on OPV2V-C. We report the performance under each corruption AP_c and the overall corruption robustness AP_{cor} averaged over all corruption types. The results are evaluated based on AP@0.7.

Cortype	AttFuse [12]	F-Cooper [1]	V2X-ViT [11]	DiscoNet [6]	V2VNet [9]	CoBEVT [10]	Max	Late	NoFusion
$\mathrm{AP}_{clean}\uparrow$	12.90	11.52	31.41	19.56	12.18	12.11	16.02	43.02	17.16
Bright	8.02	2.88	19.66	14.27	9.67	5.46	9.87	28.33	10.57
Dark	7.28	9.52	8.94	10.12	2.05	5.44	5.43	10.41	3.72
Fog	6.77	6.96	6.82	9.89	5.20	5.01	6.00	3.85	1.02
Frost	4.46	5.38	5.29	5.57	0.54	1.25	4.63	3.86	1.28
Snow	2.96	2.19	3.65	3.89	1.52	1.94	6.22	4.49	1.60
Gaussian	4.31	4.30	4.07	0.69	0.69	2.04	4.63	5.10	1.79
Impulse	4.78	4.61	4.22	0.38	0.59	1.75	4.55	5.55	1.91
Shot	3.68	5.34	4.41	0.41	0.61	1.23	4.70	6.33	2.43
Zoom	8.00	9.81	11.94	10.28	2.39	7.47	8.58	11.74	4.18
Motion	10.13	11.87	15.50	14.90	5.08	8.82	10.14	21.43	7.48
Defocus	10.58	9.79	11.39	11.99	1.95	7.04	7.46	7.86	2.72
Crash	8.89	6.73	9.12	6.73	6.10	7.86	7.72	18.18	6.46
Quant	8.84	7.06	19.30	15.39	8.34	7.18	11.75	28.00	10.94
Tempormis	10.14	9.06	24.56	15.72	8.98	10.21	12.29	23.33	17.18
$\mathrm{AP}_{cor}\uparrow$	7.06	6.82	10.63	8.59	3.84	5.19	7.43	12.75	5.23

Table 10. Benchmarking results for Ego Interference and CAV Interference on OPV2V-C. We report collaborative compensation and disruption performance under each corruption type, including NegC_c and PosC_c, as well as averages across all corruption types, mNegC and mPosC. Results are evaluated based on AP@0.3.

Cortype	AttFuse [12]		F-Cooper [1]		V2X-ViT [11]		DiscoNet [6]		V2VNet [9]		CoBEVT [10]		Max		Late	
	NegCc	PosCc	NegCc	PosCc	NegCc	PosCc	NegCc	PosCc	NegCc	PosCc	NegCc	PosCc	NegCc	PosCc	NegCc	PosCc
Bright	127.22	42.35	120.56	42.59	80.80	71.78	88.68	54.45	92.26	70.79	100.59	51.63	109.62	60.54	82.45	64.95
Dark	138.80	22.97	137.75	33.81	107.13	31.07	118.27	27.61	132.71	20.27	128.17	33.66	129.81	37.21	99.91	50.81
Gaussian	142.34	24.38	138.44	26.57	122.20	26.73	123.49	22.73	125.23	20.94	124.14	31.60	122.78	40.35	99.75	50.95
Impulse	142.28	26.86	138.68	26.08	121.87	28.24	123.33	22.17	125.07	21.04	123.43	31.21	122.13	40.17	99.53	50.99
Shot	141.23	23.98	136.98	29.35	122.98	26.10	124.20	21.85	126.14	20.86	125.13	31.80	120.01	41.50	99.89	50.84
Zoom	123.31	41.45	124.00	44.93	95.40	57.46	104.56	45.29	101.94	53.63	109.86	49.09	102.96	54.73	88.50	58.92
Motion	121.77	40.65	123.47	42.35	94.76	50.55	101.64	41.81	115.19	37.56	108.08	46.86	101.44	51.13	90.30	56.68
Defocus	123.96	38.82	125.54	38.27	102.31	44.73	113.33	32.76	119.32	27.63	111.97	40.47	109.01	44.91	101.55	50.67
Crash	119.06	45.78	122.38	43.63	93.42	40.22	110.81	30.44	106.66	39.80	99.43	50.70	108.22	50.27	91.53	56.95
Quant	121.93	31.89	119.97	37.49	97.77	43.77	95.42	34.97	102.29	41.60	107.51	36.20	111.75	44.79	98.76	49.63
mNegC$\downarrow$/mPosC$\uparrow$	130.19	33.92	128.78	36.51	103.86	42.06	110.37	33.41	114.68	35.41	113.83	40.32	113.77	46.56	95.22	54.14

Table 11. Benchmarking results for Ego Interference and CAV Interference on OPV2V-C. We report collaborative compensation and disruption performance under each corruption type, including NegC_c and PosC_c, as well as averages across all corruption types, mNegC and mPosC. Results are evaluated based on AP@0.7.

Cortype	AttFuse [12]		F-Cooper [1]		V2X-ViT [11]		DiscoNet [6]		V2VNet [9]		CoBEVT [10]		Max		Late	
	NegCc	PosCc	NegCc	PosCc	NegCc	PosCc	NegCc	PosCc	NegCc	PosCc	NegCc	PosCc	NegCc	PosCc	NegCc	PosCc
Bright	110.45	6.05	109.49	6.25	94.89	16.18	100.62	12.44	111.66	8.83	108.57	2.58	107.25	10.83	92.14	37.29
Dark	112.24	3.77	111.23	8.19	101.52	9.39	104.27	9.48	116.77	0.93	108.37	3.55	112.68	8.69	99.99	32.70
Gaussian	112.19	2.14	111.17	4.19	105.90	3.22	107.38	2.79	115.72	0.90	110.96	1.10	109.75	9.58	99.99	32.71
Impulse	112.11	2.30	111.14	3.97	105.79	3.93	107.33	2.66	115.73	0.84	111.08	1.11	109.71	9.36	99.98	32.73
Shot	112.13	2.19	110.82	5.60	105.65	3.07	107.42	2.46	116.02	0.89	111.88	1.11	109.28	9.86	99.99	32.70
Zoom	109.87	9.56	109.55	9.67	96.89	15.21	102.21	10.87	113.13	8.39	106.68	6.37	106.82	10.81	96.97	34.16
Motion	109.56	10.89	108.91	10.61	97.50	14.79	101.33	12.47	114.70	2.20	106.45	6.93	105.89	10.31	97.10	34.23
Defocus	109.91	11.32	109.28	9.28	99.69	13.01	103.84	9.44	115.51	1.51	106.41	4.12	107.59	9.51	100.51	32.56
Crash	109.72	10.32	109.45	9.24	100.51	6.87	105.35	5.86	113.70	3.26	106.88	6.62	108.00	10.85	94.81	35.33
Quant	110.59	4.49	109.08	7.85	101.17	7.04	102.17	9.75	112.88	3.68	107.50	1.99	108.39	8.25	98.74	31.92
mNegC$\downarrow$/mPosC$\uparrow$	110.88	6.30	110.01	7.49	100.95	9.27	104.19	7.82	114.58	3.14	108.48	3.55	108.54	9.80	98.02	33.63

Table 12. Detailed experimental results of AP_{cor} for CoBEVT and its variants

Cortype	CoBEVT [10]			+BN			+BN+RCP-Mix			+BN+RCP-Drop			+BN+RCP-Drop+RCP-Mix		
	APc30	APc50	APc70	APc30	APc50	APc70	APc30	APc50	APc70	APc30	APc50	APc70	APc30	APc50	APc70
Bright	41.71	23.18	5.46	63.31	39.45	12.20	67.28	42.73	12.47	66.89	44.29	12.73	70.27	49.30	17.04
Quant	44.32	25.86	7.18	54.30	32.50	9.09	59.38	37.87	11.85	56.47	36.24	10.33	57.64	39.24	13.07
Defocus	24.60	17.01	7.04	52.05	32.14	9.96	56.34	35.80	11.60	51.66	32.97	9.52	52.61	35.59	11.88
Fog	14.56	10.78	5.01	56.99	33.82	9.22	61.23	36.92	10.31	62.02	39.45	10.23	61.52	41.18	11.89
Frost	12.60	6.14	1.25	36.52	20.62	5.54	38.90	23.89	7.37	36.98	22.07	5.08	33.06	20.14	5.17
Gaussian	11.24	5.97	2.04	32.59	19.71	6.39	36.56	23.75	8.51	32.39	20.53	6.24	33.45	21.58	6.90
Impulse	10.83	5.65	1.75	33.81	20.14	6.20	37.37	24.20	8.09	35.01	21.62	6.03	35.09	21.87	6.73
Dark	21.86	14.12	5.44	39.11	23.42	7.33	44.61	28.90	9.94	40.10	25.39	7.65	38.71	25.41	7.98
Motion	36.51	24.55	8.82	56.76	34.26	9.63	61.11	38.08	11.84	59.15	37.55	10.16	60.35	40.78	13.81
Shot	9.13	4.51	1.23	34.30	20.99	6.79	36.70	23.80	8.06	34.36	21.62	6.18	34.81	22.65	7.34
Snow	18.46	9.36	1.94	49.59	28.59	7.66	51.71	31.45	9.23	50.43	30.74	7.56	49.66	30.89	8.50
Crash	38.42	23.23	7.86	28.69	16.59	4.98	31.97	19.74	6.18	32.80	20.12	5.79	32.11	21.15	7.00
Zoom	29.32	18.95	7.47	47.97	25.01	6.06	52.56	30.38	7.92	52.24	29.10	6.88	53.03	31.51	8.01
Tempormis	55.54	33.38	10.21	68.21	42.91	13.46	72.36	48.08	16.11	70.16	47.76	15.34	74.64	54.43	20.75
$\mathrm{AP}_{cor}\uparrow$	26.37	15.91	5.19	46.73	27.87	8.18	50.58	31.83	9.96	48.62	30.68	8.55	49.07	32.55	10.43

Table 13. Detailed experimental results of NegC for CoBEVT and its variants

Cortype	CoBEVT [10]			+BN			+BN+RCP-Mix			+BN+RCP-Drop			+BN+RCP-Drop+RCP-Mix		
	NegCc30	NegCc50	NegCc70	NegCc30	NegCc50	NegCc70	NegCc30	NegCc50	NegCc70	NegCc30	NegCc50	NegCc70	NegCc30	NegCc50	NegCc70
Bright	100.59	107.82	108.57	73.15	93.56	106.45	69.48	89.60	105.30	66.59	86.07	103.87	62.31	79.45	98.36
Quant	107.51	110.00	107.50	102.90	109.90	109.93	93.58	102.50	106.81	90.54	100.78	105.25	100.67	102.67	105.69
Defocus	111.97	107.82	106.41	113.00	109.20	108.27	103.24	103.44	106.64	103.18	100.72	103.36	110.04	102.97	102.56
Gaussian	124.14	117.93	110.96	137.85	123.10	111.14	143.03	125.95	113.63	155.81	132.21	115.69	157.35	131.79	113.00
Impulse	123.43	117.86	111.08	134.45	122.37	111.05	139.27	124.98	113.51	152.23	131.02	115.84	154.37	130.58	112.78
Dark	128.17	116.00	108.37	136.53	123.26	112.57	121.51	114.47	109.56	125.50	119.40	112.68	134.29	120.77	111.29
Motion	108.08	106.19	106.45	91.23	99.21	106.39	83.48	94.79	104.30	84.20	91.76	101.13	88.42	91.64	99.93
Shot	125.13	118.17	111.88	136.33	123.51	111.34	139.23	124.95	113.62	153.44	131.33	116.09	154.62	131.20	113.44
Crash	99.43	105.05	106.88	121.67	117.06	110.99	112.96	110.46	109.90	100.81	103.28	106.17	107.57	104.90	105.65
Zoom	109.86	107.98	106.68	102.92	108.19	108.82	89.61	99.95	106.27	90.24	97.98	102.87	92.57	96.36	101.27
mNegC	113.83	111.48	108.48	115.00	112.94	109.69	109.54	109.11	108.95	112.25	109.45	108.30	116.22	109.23	106.40

Table 14. Detailed experimental results of PosC for CoBEVT and its variants

Cortype	CoBEVT [10]			+BN			+BN+RCP-Mix			+BN+RCP-Drop			+BN+RCP-Drop+RCP-Mix		
	PosCc30	PosCc50	PosCc70	PosCc30	PosCc50	PosCc70	PosCc30	PosCc50	PosCc70	PosCc30	PosCc50	PosCc70	PosCc30	PosCc50	PosCc70
Bright	25.67	6.24	-1.93	48.80	24.21	4.73	52.17	28.43	4.53	53.24	31.02	5.64	54.98	34.11	7.22
Quant	33.97	12.82	1.83	40.82	17.89	2.93	47.58	24.24	4.80	42.95	20.68	3.57	45.07	25.35	5.21
Defocus	39.68	18.68	4.07	42.55	21.31	5.68	45.83	26.09	6.70	41.05	20.86	4.16	41.90	23.30	5.29
Gaussian	31.46	11.45	1.09	34.01	15.63	3.22	36.85	20.68	5.40	32.33	16.82	3.11	31.82	18.87	3.96
Impulse	31.05	11.11	1.09	35.83	16.46	3.37	38.73	22.04	5.58	34.28	17.92	3.38	33.15	19.48	4.28
Dark	33.64	14.97	3.55	35.43	15.03	2.66	39.49	20.86	5.54	37.40	17.36	2.67	36.64	20.00	4.52
Motion	38.94	19.19	5.30	43.65	20.70	4.86	47.28	25.62	5.73	43.08	20.79	2.93	45.14	24.86	5.75
Shot	31.74	11.81	1.11	35.16	16.33	3.13	38.47	21.94	5.27	33.50	17.86	3.51	33.44	19.72	3.89
Crash	40.77	18.96	3.52	38.47	17.27	3.18	40.12	20.93	4.96	40.73	19.12	1.95	42.50	22.96	4.07
Zoom	36.54	17.63	5.26	40.17	18.01	4.15	45.57	23.55	5.69	40.43	18.26	2.87	42.43	21.77	4.68
mPosC	34.35	14.29	2.49	39.49	18.28	3.79	43.21	23.44	5.42	39.90	20.07	3.38	40.71	23.04	4.89

Table 15. Detailed experimental results of AP_{cor} for AttFuse [12] and its variants

Cortype	AttFuse [12]			+BN			+BN+RCP-Mix			+BN+RCP-Drop			+BN+RCP-Drop+RCP-Mix		
	APc30	APc50	APc70	APc30	APc50	APc70	APc30	APc50	APc70	APc30	APc50	APc70	APc30	APc50	APc70
Bright	34.67	21.39	8.02	53.06	33.10	11.25	60.84	41.07	14.62	58.98	40.96	15.11	56.57	42.46	16.77
Quant	39.44	26.01	8.84	40.73	25.72	8.47	49.30	33.08	12.41	48.84	33.74	13.20	46.24	34.23	14.74
Defocus	24.11	18.64	10.58	42.98	27.03	9.46	49.14	32.32	11.77	46.01	33.57	13.01	43.58	33.03	13.30
Fog	12.33	10.30	6.77	39.03	23.49	7.47	52.91	32.39	10.39	53.38	36.44	12.59	50.80	36.28	13.25
Frost	9.44	7.12	4.46	22.42	14.08	5.26	32.81	22.25	8.90	23.28	17.91	7.80	20.10	15.58	6.87
Gaussian	11.77	9.17	4.31	25.29	16.90	6.89	28.73	21.29	10.40	22.45	17.75	9.22	17.52	14.26	7.19
Impulse	11.55	9.17	4.78	24.24	16.16	6.58	28.69	21.22	10.30	21.41	16.54	8.18	15.46	12.23	5.47
Dark	18.53	14.00	7.28	30.84	19.94	7.25	31.87	22.04	9.54	29.34	21.14	9.46	24.76	19.04	9.32
Motion	30.61	22.07	10.13	44.39	26.73	8.49	54.88	35.81	12.32	51.27	35.97	13.28	48.22	35.67	13.90
Shot	11.22	8.58	3.68	25.90	16.56	6.19	28.44	21.05	10.14	20.84	16.60	8.65	18.06	14.94	8.28
Snow	10.31	6.46	2.96	32.31	19.67	6.61	46.86	30.65	10.79	36.20	25.45	9.30	32.67	23.98	9.67
Crash	32.86	22.30	8.89	19.24	11.76	3.82	28.48	19.14	7.39	22.94	15.91	6.78	19.86	14.37	5.94
Zoom	26.07	18.85	8.00	43.64	25.78	7.11	47.41	28.39	7.97	44.00	28.59	8.57	43.40	30.23	10.37
Tempormis	48.47	29.74	10.14	57.74	35.98	11.66	63.94	43.26	15.83	66.10	45.26	17.42	66.82	49.44	21.18
$\mathrm{AP}_{cor}\uparrow$	22.96	15.99	7.06	35.84	22.35	7.61	43.16	28.85	10.91	38.93	27.56	10.90	36.00	26.84	11.16

Table 16. Detailed experimental results of NegC for AttFuse [12] and its variants

Cortype	AttFuse [12]			+BN			+BN+RCP-Mix			+BN+RCP-Droput			+BN+RCP-Mix+RCP-Drop		
	NegCc30	NegCc50	NegCc70	NegCc30	NegCc50	NegCc70	NegCc30	NegCc50	NegCc70	NegCc30	NegCc50	NegCc70	NegCc30	NegCc50	NegCc70
Bright	127.22	121.27	110.45	95.48	103.70	106.05	80.94	92.74	103.22	86.51	92.79	101.42	92.49	92.58	98.93
Quant	121.93	118.03	110.59	143.44	130.18	115.55	109.92	110.96	108.31	112.90	109.44	106.51	123.75	111.30	106.23
Defocus	123.96	118.17	109.91	125.07	117.51	111.25	108.36	105.92	107.22	121.26	110.99	106.28	125.09	111.58	104.79
Gaussian	142.34	127.32	112.19	167.46	140.66	116.01	157.90	131.30	111.32	158.12	133.10	114.49	167.05	138.28	116.14
Impulse	142.28	127.04	112.11	166.02	139.89	115.80	156.30	130.58	111.24	156.05	131.69	114.08	165.53	137.16	115.96
Dark	138.80	126.73	112.24	152.81	132.65	114.40	148.52	128.44	113.05	139.71	123.32	112.54	144.05	123.32	109.60
Motion	121.77	116.67	109.56	116.18	115.55	111.53	93.60	99.81	105.63	102.92	101.63	103.74	108.00	101.68	102.20
Shot	141.23	126.87	112.13	163.00	138.29	115.31	157.59	131.30	111.19	155.67	131.53	113.77	166.20	137.64	116.32
Crash	119.06	116.22	109.72	138.19	125.42	113.30	118.53	113.82	110.68	129.16	117.74	110.21	136.01	119.68	109.11
Zoom	123.31	117.63	109.87	114.84	116.60	111.84	99.35	104.82	107.15	103.71	104.20	104.99	106.56	102.66	102.17
mNegC	130.19	121.59	110.88	138.25	126.04	113.10	123.10	114.97	108.90	126.60	115.64	108.80	133.47	117.59	108.14

Table 17. Detailed experimental results of PosC for AttFuse [12] and its variants

Cortype	AttFuse [12]			+BN			+BN+RCP-Mix			+BN+Drop			+BN+RCP-Mix+RCP-		
	PosCc30	PosCc50	PosCc70	PosCc30	PosCc50	PosCc70	PosCc30	PosCc50	PosCc70	PosCc30	PosCc50	PosCc70	PosCc30	PosCc50	PosCc70
Bright	16.39	8.54	1.54	31.84	17.93	4.64	44.50	26.32	7.37	42.28	25.07	6.67	37.76	26.31	8.87
Quant	29.66	17.63	4.33	36.82	23.23	7.79	38.66	24.28	7.46	29.73	17.89	5.45	24.76	16.10	5.92
Defocus	38.04	25.27	11.27	39.05	24.33	8.68	41.40	27.57	10.01	36.80	24.90	8.91	30.79	21.32	8.07
Gaussian	24.24	13.30	2.13	26.90	17.19	8.47	25.09	18.10	7.65	18.84	12.96	6.81	15.71	11.81	6.85
Impulse	26.70	15.75	2.28	27.48	17.68	8.59	26.52	18.88	7.78	19.68	13.33	6.77	16.51	12.34	7.03
Dark	22.95	12.96	3.77	26.89	16.11	5.71	33.87	23.40	9.31	23.56	14.56	7.69	22.62	14.25	5.87
Motion	32.73	21.12	9.25	38.71	22.60	7.51	42.06	26.11	8.69	36.79	24.21	8.75	31.25	21.88	8.45
Shot	23.92	13.12	2.19	27.92	17.67	8.30	25.47	18.32	7.50	20.14	13.63	6.33	16.18	12.44	6.37
Crash	35.86	22.35	7.22	24.84	13.35	3.05	31.49	19.44	5.17	26.20	15.87	5.54	25.25	15.89	4.71
Zoom	28.90	19.66	8.44	34.23	18.46	5.95	38.72	22.65	7.94	31.91	19.23	7.77	29.26	19.72	7.99
mPosC	27.94	16.97	5.24	31.47	18.85	6.87	34.78	22.51	7.89	28.59	18.17	7.07	25.01	17.21	7.01

Table 18. Benchmarking results for Global Interference on V2XSet-C. We report the performance under each corruption RCE and the overall corruption robustness mRCE averaged over all corruption types. The results are evaluated based on AP@0.5.

Cortype	AttFuse [12]	F-Cooper [1]	V2X-ViT [11]	V2VNet [9]	CoBEVT [10]	Max	Late	NoFusion
$\mathrm{AP}_{clean}\uparrow$	38.51	49.54	50.35	30.62	47.85	45.42	54.02	29.89
Bright	35.54	36.01	25.05	41.48	47.34	26.11	20.60	28.60
Dark	67.42	72.76	63.24	69.73	63.59	66.49	81.21	88.97
Fog	75.28	69.55	55.67	65.37	65.59	83.91	90.46	95.00
Frost	65.98	83.22	77.80	82.59	85.26	69.89	74.60	83.74
Snow	66.77	78.88	70.93	93.42	81.89	76.01	76.85	84.16
Gaussian	89.12	96.88	67.12	87.49	88.14	78.36	89.76	93.10
Impulse	91.92	98.54	68.25	89.93	90.68	82.00	93.56	96.08
Shot	89.81	94.23	64.23	87.66	87.13	76.84	87.29	90.76
Zoom	39.26	60.29	45.41	71.49	51.21	46.13	65.21	69.88
Motion	30.62	47.75	40.78	61.66	38.47	22.30	45.06	50.41
Defocus	43.00	69.21	73.45	84.00	67.76	43.20	74.39	77.46
Crash	49.59	64.47	54.15	61.36	67.14	67.84	50.86	56.61
Quant	40.49	41.49	33.93	41.25	41.24	37.29	41.17	44.54
Tempormis	8.13	8.78	11.00	7.12	11.73	12.31	0.00	0.00
$\mathrm{mRCE}\downarrow$	56.64	65.86	53.64	67.47	63.37	56.33	63.64	68.52

Table 19. Benchmarking results for Global Interference on V2XSet-C. We report the performance under each corruption AP_c and the overall corruption robustness AP_{cor} averaged over all corruption types. The results are evaluated based on AP@0.5.

Cortype	AttFuse [12]	F-Cooper [1]	V2X-ViT [11]	V2VNet [9]	CoBEVT [10]	Max	Late	NoFusion
$\mathrm{AP}_{clean}\uparrow$	38.51	49.54	50.35	30.62	47.85	45.42	54.02	29.89
Bright	24.82	31.7	37.74	17.92	25.2	33.56	42.89	21.34
Dark	12.55	13.50	18.51	9.27	17.42	15.22	10.15	3.30
Fog	9.52	15.08	22.32	10.60	16.46	7.31	5.15	1.49
Frost	13.1	8.31	11.18	5.33	7.05	13.68	13.72	4.86
Snow	12.80	10.46	14.64	2.02	8.67	10.89	12.51	4.74
Gaussian	4.19	1.55	16.55	3.83	5.68	9.83	5.53	2.06
Impulse	3.11	0.72	15.98	3.08	4.46	8.18	3.48	1.17
Shot	3.92	2.86	18.01	3.78	6.16	10.52	6.86	2.76
Zoom	23.39	19.67	27.49	8.73	23.35	24.47	18.79	9.00
Motion	26.72	25.89	29.82	11.74	29.44	35.29	29.68	14.82
Defocus	21.95	15.25	13.37	4.9	15.43	25.8	13.84	6.74
Crash	19.41	17.6	23.09	11.83	15.72	14.61	26.55	12.97
Quant	22.92	28.98	33.27	17.99	28.12	28.48	31.78	16.58
Tempormis	35.38	45.19	44.81	28.44	42.24	39.83	29.89	29.89
$\mathrm{AP}_{cor}\uparrow$	16.69	16.91	23.34	9.96	17.52	19.83	17.91	9.40

Table 20. Benchmarking results for Global Interference on V2XSet-C. We report the performance under each corruption RCE and the overall corruption robustness mRCE averaged over all corruption types. The results are evaluated based on AP@0.3.

Cortype	AttFuse [12]	F-Cooper [1]	V2X-ViT [11]	V2VNet [9]	CoBEVT [10]	Max	Late	NoFusion
$\mathrm{AP}_{clean}\uparrow$	50.29	62.58	69.16	53.25	66.41	60.97	69.04	43.75
Bright	32.48	32.97	22.22	39.76	40.19	21.87	20.60	28.59
Dark	73.54	72.54	66.18	75.06	64.64	65.11	81.21	86.60
Fog	79.87	73.56	58.32	69.69	66.32	84.20	90.46	93.37
Frost	70.15	82.76	75.29	85.13	80.85	71.95	74.60	78.22
Snow	70.70	79.03	71.65	93.34	77.18	75.93	76.85	77.29
Gaussian	90.47	91.98	72.26	88.04	86.32	75.78	89.76	91.65
Impulse	93.09	94.57	72.87	90.66	89.06	79.79	93.56	94.73
Shot	90.81	88.90	68.14	87.31	84.93	73.80	87.29	90.15
Zoom	44.42	55.77	40.01	69.69	47.33	38.63	65.21	58.24
Motion	34.78	45.78	38.32	61.80	37.38	24.82	45.06	47.67
Defocus	47.08	65.48	69.55	84.12	64.85	43.77	74.39	71.41
Crash	48.86	61.67	49.27	60.85	62.80	63.61	50.86	54.80
Quant	33.88	38.92	29.57	36.85	34.61	33.99	41.17	41.15
Tempormis	5.13	9.65	7.43	5.46	11.29	7.58	0.00	0.00
$\mathrm{mRCE}\downarrow$	58.23	63.83	52.94	67.70	60.55	54.35	63.64	65.28

Table 21. Benchmarking results for Global Interference on V2XSet-C. We report the performance under each corruption AP_c and the overall corruption robustness AP_{cor} averaged over all corruption types. The results are evaluated based on AP@0.3.

Cortype	AttFuse [12]	F-Cooper [1]	V2X-ViT [11]	V2VNet [9]	CoBEVT [10]	Max	Late	NoFusion
$\mathrm{AP}_{clean}\uparrow$	50.29	62.58	69.16	53.25	66.41	60.97	69.04	43.75
Bright	33.96	41.95	53.79	32.08	39.72	47.63	42.89	31.24
Dark	13.31	17.18	23.39	13.28	23.48	21.27	10.15	5.86
Fog	10.12	16.55	28.83	16.14	22.37	9.63	5.15	2.90
Frost	15.01	10.79	17.09	7.92	12.72	17.1	13.72	9.53
Snow	14.73	13.12	19.60	3.54	15.16	14.67	12.51	9.94
Gaussian	4.79	5.02	19.18	6.37	9.08	14.76	5.53	3.65
Impulse	3.47	3.40	18.76	4.97	7.27	12.32	3.48	2.30
Shot	4.62	6.94	22.04	6.76	10.08	15.97	6.86	4.31
Zoom	27.95	27.68	41.49	16.14	34.98	37.42	18.79	18.27
Motion	32.8	33.93	42.66	20.34	41.59	45.84	29.68	22.90
Defocus	26.61	21.60	21.06	8.46	23.35	34.28	13.84	12.51
Crash	25.72	23.99	35.09	20.85	24.70	22.19	26.55	19.78
Quant	33.25	38.22	48.71	33.63	43.42	40.24	31.78	25.75
Tempormis	47.71	56.54	64.02	50.34	58.91	56.35	29.89	43.75
$\mathrm{AP}_{cor}\uparrow$	21.00	22.63	32.54	17.20	26.20	27.83	17.91	15.19

Table 22. Benchmarking results for Global Interference on V2XSet-C. We report the performance under each corruption RCE and the overall corruption robustness mRCE averaged over all corruption types. The results are evaluated based on AP@0.7.

Cortype	AttFuse [12]	F-Cooper [1]	V2X-ViT [11]	V2VNet [9]	CoBEVT [10]	Max	Late	NoFusion
$\mathrm{AP}_{clean}\uparrow$	16.05	21.49	23.44	6.81	15.18	17.72	25.09	12.54
Bright	35.46	37.26	36.89	28.90	53.61	40.76	29.92	43.91
Dark	42.19	61.10	50.69	45.90	52.62	56.55	87.29	93.54
Fog	50.97	52.98	49.51	40.65	61.45	80.77	94.72	97.74
Frost	45.12	80.10	74.04	78.21	89.86	63.04	84.90	91.31
Snow	42.72	74.25	69.25	90.81	85.67	74.00	87.36	92.09
Gaussian	79.18	97.24	51.25	78.74	89.47	71.91	92.72	95.44
Impulse	83.79	99.06	51.86	82.11	91.00	79.39	96.27	98.17
Shot	81.53	96.18	50.06	83.47	89.12	77.18	90.14	92.06
Zoom	33.50	72.59	51.60	75.33	50.87	56.26	84.90	87.54
Motion	23.95	50.25	44.80	17.62	34.33	22.45	61.40	69.17
Defocus	29.18	71.53	75.14	87.67	67.87	40.59	83.91	88.31
Crash	52.26	76.00	65.30	67.02	74.40	76.79	52.96	59.36
Quant	33.37	41.81	-12.60	45.11	50.71	40.54	47.94	48.66
Tempormis	7.33	9.50	12.67	8.14	12.24	15.93	0.00	0.00
$\mathrm{mRCE}\downarrow$	45.75	65.70	-41.20	59.26	64.52	56.87	71.03	75.52

Table 23. Benchmarking results for Global Interference on V2XSet-C. We report the performance under each corruption AP_c and the overall corruption robustness AP_{cor} averaged over all corruption types. The results are evaluated based on AP@0.7.

Cortype	AttFuse [12]	F-Cooper [1]	V2X-ViT [11]	V2VNet [9]	CoBEVT [10]	Max	Late	NoFusion
$\mathrm{AP}_{clean}\uparrow$	16.05	21.49	23.44	6.81	15.18	17.72	25.09	12.54
Bright	10.36	13.48	14.79	4.84	7.04	10.49	17.58	7.03
Dark	9.28	8.36	11.56	3.68	7.19	7.7	3.19	0.81
Fog	7.87	10.10	11.84	4.04	5.85	3.41	1.32	0.28
Frost	8.81	4.28	6.09	1.48	1.54	6.55	3.79	1.09
Snow	9.19	5.53	7.21	0.63	2.18	4.61	3.17	0.99
Gaussian	3.34	0.59	11.43	1.45	1.60	4.98	1.83	0.57
Impulse	2.60	0.20	11.28	1.22	1.37	3.65	0.94	0.23
Shot	2.96	0.82	11.71	1.13	1.65	4.04	2.47	1.00
Zoom	10.67	5.89	11.34	1.68	7.46	7.75	3.79	1.56
Motion	12.21	10.69	12.94	5.61	9.97	13.74	9.68	3.87
Defocus	11.37	6.12	5.83	0.84	4.88	10.53	4.04	1.47
Crash	7.66	5.16	8.13	2.25	3.89	4.11	11.80	5.10
Quant	10.69	12.51	31.87	3.74	7.48	10.54	13.06	6.44
Tempormis	14.87	19.45	20.47	6.26	13.32	14.80	12.54	12.54
$\mathrm{AP}_{cor}\uparrow$	8.71	7.37	33.10	2.77	5.39	7.64	6.37	3.07

Table 24. Benchmarking results for Ego Interference and CAV Interference on V2XSet-C. We report collaborative compensation and disruption performance under each corruption type, including NegC_c and PosC_c, as well as averages across all corruption types, mNegC and mPosC. Results are evaluated based on AP@0.3.

Cortype	AttFuse [12]		F-Cooper [1]		V2X-ViT [11]		V2VNet [9]		CoBEVT [10]		Max		Late	
	NegCc	PosCc	NegCc	PosCc	NegCc	PosCc	NegCc	PosCc	NegCc	PosCc	NegCc	PosCc	NegCc	PosCc
Bright	103.04	7.51	87.70	14.21	75.22	27.23	107.47	1.27	97.92	5.61	98.22	30.63	78.18	34.17
Dark	115.57	22.39	112.75	21.66	93.71	34.36	127.13	12.35	95.96	35.05	96.74	23.66	99.97	35.58
Gaussian	119.63	4.39	137.78	4.71	104.68	33.29	129.96	9.86	98.57	13.28	102.04	17.56	100.00	35.57
Impulse	119.50	4.47	135.47	4.33	105.08	33.31	130.06	9.46	97.82	12.97	102.01	19.11	100.00	35.58
Shot	118.35	5.03	130.22	4.13	99.96	36.27	127.57	8.73	98.67	13.45	101.28	14.11	100.01	35.56
Zoom	110.77	26.59	91.36	33.93	75.40	42.31	116.30	12.25	95.75	39.38	98.10	35.58	93.92	34.08
Motion	104.60	25.38	93.74	32.45	76.20	36.47	120.60	2.90	93.62	37.45	94.82	40.55	92.91	33.42
Defocus	106.79	29.11	97.37	29.76	91.18	27.95	126.86	3.88	95.06	28.52	95.43	37.24	103.81	32.36
Crash	104.94	20.55	92.75	15.44	81.48	32.27	106.10	6.37	99.52	13.57	98.32	12.58	91.76	35.38
Quant	109.46	20.86	99.02	18.31	83.93	30.81	108.27	9.08	96.54	23.74	97.71	23.99	98.56	30.49
$\mathrm{mNegC}\downarrow/\mathrm{mPosC}\uparrow$	111.27	16.63	107.82	17.89	88.68	33.43	120.03	7.62	96.94	22.30	98.47	25.50	95.91	34.22

Table 25. Benchmarking results for Ego Interference and CAV Interference on V2XSet-C. We report collaborative compensation and disruption performance under each corruption type, including NegC_c and PosC_c, as well as averages across all corruption types, mNegC and mPosC. Results are evaluated based on AP@0.5.

Cortype	AttFuse [12]		F-Cooper [1]		V2X-ViT [11]		V2VNet [9]		CoBEVT [10]		Max		Late	
	NegCc	PosCc	NegCc	PosCc	NegCc	PosCc	NegCc	PosCc	NegCc	PosCc	NegCc	PosCc	NegCc	PosCc
Bright	99.16	7.07	87.31	13.91	85.41	15.00	110.20	-1.67	93.95	-0.51	88.93	22.45	78.18	34.17
Dark	103.92	19.56	101.08	17.01	92.48	23.36	118.27	10.72	92.84	21.29	97.97	14.29	99.97	35.58
Gaussian	110.04	2.95	124.33	1.03	97.12	23.75	120.61	4.59	97.43	6.51	106.69	10.97	100.00	35.57
Impulse	110.13	3.00	122.76	0.94	97.08	24.20	120.01	4.69	96.36	6.38	107.07	11.43	100.00	35.58
Shot	109.33	3.42	117.12	1.77	94.64	23.97	119.68	2.84	97.46	6.62	106.46	9.18	100.01	35.56
Zoom	101.07	25.96	90.02	27.33	83.90	27.69	112.38	10.62	89.73	24.43	91.21	27.30	93.92	34.08
Motion	97.76	23.68	91.80	24.76	85.09	24.32	114.49	1.97	87.72	22.62	87.15	31.82	92.91	33.42
Defocus	100.23	25.19	93.95	20.95	94.65	16.51	118.39	2.07	94.02	14.86	90.69	27.07	103.81	32.36
Crash	99.19	16.00	89.90	10.35	88.92	18.61	108.49	2.63	94.41	6.96	97.20	7.01	91.76	35.38
Quant	101.85	14.86	93.42	13.52	90.89	19.70	110.03	3.45	92.61	11.01	99.04	15.47	98.56	30.49
$\mathrm{mNegC}\downarrow/\mathrm{mPosC}\uparrow$	103.27	14.17	101.17	13.16	91.02	21.71	115.25	4.19	93.65	12.02	97.24	17.70	95.91	34.22

Table 26. Benchmarking results for Ego Interference and CAV Interference on V2XSet-C. We report collaborative compensation and disruption performance under each corruption type, including NegC_c and PosC_c, as well as averages across all corruption types, mNegC and mPosC. Results are evaluated based on AP@0.7.

Cortype	AttFuse [12]		F-Cooper [1]		V2X-ViT [11]		V2VNet [9]		CoBEVT [10]		Max		Late	
	NegCc	PosCc	NegCc	PosCc	NegCc	PosCc	NegCc	PosCc	NegCc	PosCc	NegCc	PosCc	NegCc	PosCc
Bright	98.69	1.29	94.65	7.47	93.65	2.29	108.70	-1.21	97.92	-1.71	98.22	4.63	93.76	15.48
Dark	97.95	9.34	98.17	6.18	94.97	11.51	109.76	7.49	95.96	4.66	96.74	2.95	99.99	16.16
Gaussian	100.82	0.42	107.84	0.12	95.77	11.79	110.31	1.92	98.57	0.62	102.04	0.82	100.00	16.16
Impulse	100.83	0.42	107.37	0.11	95.59	11.76	110.51	2.12	97.82	0.62	102.01	0.91	100.00	16.16
Shot	100.47	0.46	106.20	0.19	94.73	11.71	110.16	1.17	98.67	0.65	101.28	0.73	100.00	16.16
Zoom	98.91	10.92	95.12	8.34	92.66	11.16	108.96	3.35	95.75	4.34	98.10	7.31	99.50	15.03
Motion	97.42	10.72	95.19	8.59	93.77	10.58	109.56	0.86	93.62	3.76	94.82	9.59	98.88	14.72
Defocus	97.54	10.65	95.69	4.98	96.51	1.90	110.13	0.24	95.06	2.04	95.43	6.09	101.23	14.59
Crash	98.30	3.43	94.67	1.09	95.27	3.95	108.15	-1.06	99.52	-0.48	98.32	-0.41	96.55	15.87
Quant	97.88	4.25	95.28	3.83	96.07	3.41	108.38	0.88	96.54	1.43	97.71	2.81	100.05	14.03
$\mathrm{mNegC}\downarrow/\mathrm{mPosC}\uparrow$	98.88	5.19	99.02	4.09	94.90	8.01	109.46	1.58	96.94	1.59	98.47	3.54	98.99	15.44

Table 27. Benchmarking results for Global Interference on DAIR-V2X-C. We report the performance under each corruption RCE and the overall corruption robustness mRCE averaged over all corruption types. The results are evaluated based on AP@0.5.

RCE50	AttFuse [12]	F-Cooper [1]	V2X-ViT [11]	DiscoNet [6]	V2VNet [9]	CoBEVT [10]	Max	Late	NoFusion
$\mathrm{AP}_{clean}\uparrow$	1.72	2.62	5.76	2.13	4.26	4.25	2.14	4.84	1.66
Bright	61.51	60.08	57.36	54.27	52.02	50.68	47.12	46.16	70.00
Dark	96.16	98.70	98.16	97.84	98.97	99.86	96.54	89.26	99.88
Fog	90.23	97.33	91.77	90.33	97.09	95.20	85.40	71.69	89.52
Frost	90.23	96.79	92.92	94.65	94.93	93.55	89.05	81.40	98.19
Snow	83.84	90.38	94.72	91.27	83.76	82.16	81.75	86.74	94.82
Gaussian	36.40	36.49	48.92	33.99	30.56	24.66	29.34	21.53	34.34
Impulse	37.67	34.43	50.83	32.77	30.05	22.16	28.78	21.82	33.49
Shot	25.81	31.30	46.60	33.24	27.89	25.32	21.57	15.62	26.87
Zoom	86.63	88.17	83.99	80.75	94.04	91.34	85.49	62.77	57.59
Motion	25.47	28.32	31.35	17.37	25.26	26.92	14.83	5.45	26.02
Defocus	41.05	38.24	32.64	26.57	39.11	35.01	21.76	4.59	22.17
Quant	27.44	34.89	32.40	32.21	31.50	30.35	28.69	27.23	32.53
Tempormis	23.95	33.21	21.11	26.48	22.44	20.61	37.67	7.11	0.00
$\mathrm{mRCE}\downarrow$	52.01	55.07	56.32	50.99	52.28	50.15	47.87	39.01	49.08

Table 28. Benchmarking results for Global Interference on DAIR-V2X-C. We report the performance under each corruption AP_C and the overall corruption robustness AP_{cor} averaged over all corruption types. The results are evaluated based on AP@0.5.

APcor50	AttFuse [12]	F-Cooper [1]	V2X-ViT [11]	DiscoNet [6]	V2VNet [9]	CoBEVT [10]	Max	Late	NoFusion
$\mathrm{AP}_{clean}\uparrow$	1.72	2.62	5.76	2.13	4.26	4.25	2.14	4.84	1.66
Bright	0.66	1.05	2.46	0.97	2.04	2.10	1.13	2.61	0.50
Dark	0.07	0.03	0.11	0.05	0.04	0.01	0.07	0.52	0.00
Fog	0.17	0.07	0.47	0.21	0.12	0.20	0.31	1.37	0.17
Frost	0.17	0.08	0.41	0.11	0.22	0.27	0.23	0.90	0.03
Snow	0.28	0.25	0.30	0.19	0.69	0.76	0.39	0.64	0.09
Gaussian	1.09	1.66	2.94	1.41	2.96	3.20	1.51	3.80	1.09
Impulse	1.07	1.72	2.83	1.43	2.98	3.31	1.52	3.78	1.10
Shot	1.28	1.80	3.08	1.42	3.07	3.17	1.68	4.08	1.21
Zoom	0.23	0.31	0.92	0.41	0.25	0.37	0.31	1.80	0.70
Motion	1.28	1.88	3.95	1.76	3.18	3.11	1.82	4.58	1.23
Defocus	1.01	1.62	3.88	1.56	2.59	2.76	1.67	4.62	1.29
Quant	1.25	1.71	3.89	1.44	2.92	2.96	1.52	3.52	1.12
Tempormis	1.31	1.75	4.54	1.57	3.30	3.37	1.33	4.50	0.00
$\mathrm{AP}_{cor}\uparrow$	0.83	1.18	2.54	1.05	2.05	2.13	1.12	2.97	0.73

Table 29. Benchmarking results for Global Interference on DAIR-V2X-C. We report the performance under each corruption RCE and the overall corruption robustness mRCE averaged over all corruption types. The results are evaluated based on AP@0.3.

RCE30	AttFuse [12]	F-Cooper [1]	V2X-ViT [11]	DiscoNet [6]	V2VNet [9]	CoBEVT [10]	Max	Late	NoFusion
$\mathrm{AP}_{clean}\uparrow$	8.35	11.60	19.80	9.49	17.50	18.20	10.10	13.10	5.07
Bright	59.19	59.61	47.55	54.42	51.24	48.12	45.95	46.16	57.08
Dark	96.31	99.19	97.00	97.70	98.65	99.64	96.89	89.26	99.88
Fog	94.40	96.72	89.09	93.49	96.37	94.24	92.88	71.69	85.33
Frost	92.38	96.66	90.29	92.86	94.12	90.73	89.85	81.40	97.20
Snow	85.41	89.91	91.90	86.39	81.71	78.19	84.51	86.74	93.85
Gaussian	35.50	34.15	42.41	31.74	31.40	27.37	28.60	21.53	30.10
Impulse	35.59	31.99	43.30	30.47	30.62	25.44	28.84	21.82	30.45
Shot	29.17	28.39	38.44	30.20	28.74	26.04	21.26	15.62	24.22
Zoom	90.83	81.87	79.57	83.67	92.76	89.16	84.33	62.77	50.49
Motion	29.22	24.50	20.47	22.21	42.82	21.99	16.22	5.45	16.17
Defocus	43.54	31.40	22.58	32.62	37.27	31.60	22.21	4.59	20.39
Quant	30.30	33.04	28.76	32.08	30.94	29.96	28.25	27.23	34.04
Tempormis	14.95	16.67	13.66	14.63	16.87	14.93	16.70	7.11	0.00
$\mathrm{mRCE}\downarrow$	53.22	52.55	51.77	50.85	53.64	49.69	47.61	39.60	46.02

Table 30. Benchmarking results for Global Interference on DAIR-V2X-C. We report the performance under each corruption AP_c and the overall corruption robustness AP_{cor} averaged over all corruption types. The results are evaluated based on AP@0.3.

APcor30	AttFuse [12]	F-Cooper [1]	V2X-ViT [11]	DiscoNet [6]	V2VNet [9]	CoBEVT [10]	Max	Late	NoFusion
$\mathrm{AP}_{clean}\uparrow$	8.35	11.60	19.80	9.49	17.50	18.20	10.10	13.10	5.07
Bright	3.41	4.67	10.40	4.33	8.51	9.46	5.45	2.61	2.18
Dark	0.31	0.09	0.59	0.22	0.24	0.07	0.31	0.52	0.01
Fog	0.47	0.38	2.16	0.62	0.63	1.05	0.72	1.37	0.74
Frost	0.64	0.39	1.92	0.68	1.03	1.69	1.02	0.90	0.14
Snow	1.22	1.17	1.61	1.29	3.19	3.98	1.56	0.64	0.31
Gaussian	5.39	7.62	11.41	6.48	11.98	13.24	7.20	3.80	3.54
Impulse	5.38	7.87	11.24	6.60	12.11	13.59	7.18	3.78	3.53
Shot	5.91	8.29	12.20	6.62	12.44	13.48	7.94	4.08	3.84
Zoom	0.77	2.10	4.05	1.55	1.26	1.98	1.58	1.80	2.51
Motion	5.91	8.74	15.76	7.38	9.98	14.22	8.45	4.58	4.25
Defocus	4.71	7.94	15.34	6.39	10.95	12.47	7.84	4.62	4.04
Quant	5.82	7.75	14.12	6.45	12.06	12.77	7.24	3.52	3.34
Tempormis	7.10	9.64	17.11	8.10	14.51	15.51	8.40	4.50	0.00
$\mathrm{AP}_{cor}\uparrow$	3.96	5.59	9.84	4.73	8.32	9.41	5.36	3.56	2.39

Table 31. Benchmarking results for Ego Interference and CAV Interference on DAIR-V2X-C. We report collaborative compensation and disruption performance under each corruption type, including NegC_c and PosC_c, as well as averages across all corruption types, mNegC and mPosC. Results are evaluated based on AP@0.3.

Cortype	AttFuse [12]		F-Cooper [1]		V2X-ViT [11]		DiscoNet [6]		V2VNet [9]		CoBEVT [10]		Max		Late	
	NegCc	PosCc	NegCc	PosCc	NegCc	PosCc	NegCc	PosCc	NegCc	PosCc	NegCc	PosCc	NegCc	PosCc	NegCc	PosCc
Bright	103.31	-0.04	102.90	4.44	99.76	11.50	101.44	1.66	100.33	8.52	100.22	10.31	100.52	8.21	97.23	14.10
Quant	102.71	-1.33	102.35	2.63	99.47	7.79	102.41	0.14	100.82	5.92	102.68	5.69	103.07	4.03	99.60	10.22
Defocus	101.95	1.17	98.07	5.23	90.67	13.37	99.77	3.07	94.98	9.50	94.93	11.74	98.20	5.79	92.11	13.13
Gaussian	100.56	0.34	100.58	3.85	99.26	9.27	100.03	1.04	96.99	8.07	98.09	9.83	100.43	5.80	95.82	12.82
Impulse	100.31	0.52	99.63	4.01	98.64	9.32	99.61	1.41	96.59	8.59	96.70	10.25	99.95	5.72	95.77	12.97
Dark	103.14	3.65	103.12	7.25	102.34	10.22	102.49	5.69	101.38	15.06	103.27	12.21	103.76	6.30	100.00	12.24
Motion	100.06	1.80	96.92	5.51	89.91	13.17	98.26	3.69	93.34	10.77	92.06	12.25	97.10	5.91	92.45	13.44
Shot	99.27	0.59	98.42	3.90	95.65	9.35	98.67	1.24	94.61	8.13	96.71	10.17	96.88	5.25	94.26	12.37
Zoom	102.89	1.76	102.34	5.59	99.92	12.35	102.00	3.48	101.32	8.77	101.75	10.75	103.02	6.66	97.98	12.58
$\mathrm{mNegC}\downarrow$/$\mathrm{mPosC}\uparrow$	101.58	0.94	100.48	4.71	97.29	10.70	100.52	2.38	97.82	9.26	98.49	10.36	100.33	5.96	96.13	12.65

Table 32. Benchmarking results for Ego Interference and CAV Interference on DAIR-V2X-C. We report collaborative compensation and disruption performance under each corruption type, including NegC_c and PosC_c, as well as averages across all corruption types, mNegC and mPosC. Results are evaluated based on AP@0.5.

Cortype	AttFuse [12]		F-Cooper [1]		V2X-ViT [11]		DiscoNet [6]		V2VNet [9]		CoBEVT [10]		Max		Late	
	NegCc	PosCc	NegCc	PosCc	NegCc	PosCc	NegCc	PosCc	NegCc	PosCc	NegCc	PosCc	NegCc	PosCc	NegCc	PosCc
Bright	101.16	-0.31	100.86	0.58	100.18	2.94	100.38	-0.20	100.49	1.92	100.51	1.95	100.45	1.55	99.37	3.03
Quant	101.01	-0.94	100.72	-0.55	100.25	1.46	100.75	-0.79	100.69	0.58	101.00	0.53	101.12	0.46	99.87	2.19
Defocus	100.81	-0.37	100.07	0.51	98.21	3.28	100.02	0.07	99.28	1.90	99.31	1.95	100.14	0.70	96.58	2.47
Gaussian	100.53	-0.64	100.22	0.07	100.12	1.92	100.24	-0.67	99.65	1.38	99.77	1.40	100.65	0.89	98.13	2.55
Impulse	100.45	-0.64	100.06	0.07	99.94	1.92	100.18	-0.64	99.58	1.57	99.38	1.51	100.49	0.92	98.17	2.67
Dark	101.06	0.73	100.87	1.17	100.86	2.53	100.76	1.00	100.66	3.78	101.19	2.65	101.26	0.99	100.00	2.66
Motion	100.55	-0.17	99.83	0.64	97.90	3.26	99.75	0.23	98.88	2.32	98.74	2.18	99.89	0.94	96.92	2.82
Shot	100.23	-0.56	99.74	0.14	99.31	1.94	99.91	-0.59	99.08	1.43	99.49	1.53	99.85	0.65	97.78	2.40
Zoom	101.02	-0.09	100.85	0.69	100.38	2.78	100.54	0.20	100.65	1.81	100.78	1.86	101.12	1.20	99.47	2.64
$\mathrm{mNegC}\downarrow$/$\mathrm{mPosC}\uparrow$	100.76	-0.33	100.36	0.37	99.68	2.45	100.28	-0.15	99.89	1.86	100.02	1.73	100.55	0.92	98.48	2.60

Table 33. Benchmarking results for Global Interference on OPV2V-C. We report the Map-view segmentationon. We report IoU for all classes performance under each corruption and the overall corruption robustness averaged over all corruption types.

Cortype	V2VNet [9]			AttFuse [12]			CoBEVT [10]			DiscoNet [6]			F-Cooper [1]		
	Road	Lane	Dynamic	Road	Lane	Dynamic	Road	Lane	Dynamic	Road	Lane	Dynamic	Road	Lane	Dynamic
Clean	44.83	30.58	34.14	45.13	32.63	35.28	51.84	37.19	47.96	45.1	28.87	28.9	49.22	35.66	50.56
Bright	32.648	21.192	28.486	28.004	15.702	20.558	34.076	21.92	34.016	29.284	13.442	17.134	38.208	24.922	43.672
Quant	32.806	19.096	25.972	25.496	15.112	18.678	37.932	22.482	32.874	33.114	16.898	16.382	36.322	21.004	36.93
Defocus	20.524	9.336	8.816	22.976	11.268	9.902	16.936	10.838	11.85	23.698	12.138	6.14	19.52	12.66	25.59
Fog	18.085	11.326	5.127	22.408	12.656	9.144	25.317	8.825	9.383	27.724	13.315	7.041	20.133	12.261	34.956
Frost	19.982	11.626	15.932	22.668	11.37	13.87	17.728	5.644	19.028	15.398	8.226	0.9	28.746	12.26	25.2
Gaussian	14.584	8.918	19.06	21.928	13.012	19.15	10.286	4.59	11.334	20.014	7.484	1.732	20.98	10.014	8.328
Impulse	12.596	7.496	17.694	55.866	12.97	19.052	19.906	2.844	7.998	19.337	4.756	1.029	20.03	8.573	5.867
Dark	16.796	5.608	4.61	21.322	8.36	5.674	19.684	8.396	0.618	16.99	5.178	4.43	19.162	2.442	24.528
Motion	23.06	12.254	15.714	24.006	12.488	13.858	28.868	14.266	21.66	30.392	15.582	12.338	23.704	16.19	32.542
Shot	15.04	9.414	18.71	21.47	12.448	19.224	10.066	4.092	9.73	20.146	4.036	1.676	19.086	9.008	7.34
Snow	17.61	9.972	15.368	15.032	9.064	12.824	7.186	3.262	8.904	19.268	1.112	0.128	21.27	9.304	19.288
Crash	25.778	14.518	19.046	22.748	14.422	15.572	27.996	17.018	15.232	31.092	14.732	9.434	32.56	15.064	33.65
Zoom	21.016	11.228	8.876	25.036	13.016	11.09	28.844	14.804	13.788	25.86	13.584	6.792	19.696	13.972	29.188

Table 34. Benchmarking results for Global Interference on OPV2V-C. We report the Map-view segmentationon. We report relative IoU for all classes performance under each corruption and the overall corruption robustness averaged over all corruption types.

Cortype	V2VNet [9]			AttFuse [12]			CoBEVT [10]			DiscoNet [6]			F-Cooper [1]		
	Road	Lane	Dynamic	Road	Lane	Dynamic	Road	Lane	Dynamic	Road	Lane	Dynamic	Road	Lane	Dynamic
Clean	44.83	30.58	34.14	45.13	32.63	35.28	51.84	37.19	47.96	45.1	28.87	28.9	49.22	35.66	50.56
Bright	27.17	30.70	16.56	37.95	51.88	41.73	34.27	41.06	29.07	35.07	53.44	40.71	22.37	30.11	13.62
Quant	26.82	37.55	23.93	43.51	53.69	47.06	26.83	39.55	31.46	26.58	41.47	43.31	26.20	41.10	26.96
Defocus	54.22	69.47	74.18	49.09	65.47	71.93	67.33	70.86	75.29	47.45	57.96	78.75	60.34	64.50	49.39
Fog	59.66	62.96	84.98	50.35	61.21	74.08	51.16	76.27	80.44	38.53	53.88	75.64	59.10	65.62	30.86
Frost	55.43	61.98	53.33	49.77	65.15	60.69	65.80	84.82	60.33	65.86	71.51	96.89	41.60	65.62	50.16
Gaussian	67.47	70.84	44.17	51.41	60.12	45.72	80.16	87.66	76.37	55.62	74.08	94.01	57.38	71.92	83.53
Impulse	71.90	75.49	48.17	-23.79	60.25	46.00	61.60	92.35	83.32	57.12	83.53	96.44	59.31	75.96	88.40
Dark	62.53	81.66	86.50	52.75	74.38	83.92	62.03	77.42	98.71	62.33	82.06	84.67	61.07	93.15	51.49
Motion	48.56	59.93	53.97	46.81	61.73	60.72	44.31	61.64	54.84	32.61	46.03	57.31	51.84	54.60	35.64
Shot	66.45	69.22	45.20	52.43	61.85	45.51	80.58	89.00	79.71	55.33	86.02	94.20	61.22	74.74	85.48
Snow	60.72	67.39	54.99	66.69	72.22	63.65	86.14	91.23	81.43	57.28	96.15	99.56	56.79	73.91	61.85
Crash	42.50	52.52	44.21	49.59	55.80	55.86	46.00	54.24	68.24	31.06	48.97	67.36	33.85	57.76	33.45
Zoom	53.12	63.28	74.00	44.52	60.11	68.57	44.36	60.19	71.25	42.66	52.95	76.50	59.98	60.82	42.27

References

[1] Qi Chen, Xu Ma, Sihai Tang, Jingda Guo, Qing Yang, and Song Fu. F-cooper: Feature based cooperative perception for autonomous vehicle edge computing system using 3d point clouds. In *Proceedings of the 4th ACM/IEEE Symposium on Edge Computing*, pages 88–100, 2019. 9, 11, 12, 13, 16, 17, 18, 19, 20, 21, 22, 23

[2] Martin Hahner, Christos Sakaridis, Dengxin Dai, and Luc Van Gool. Fog simulation on real lidar point clouds for 3d object detection in adverse weather. In *Proceedings of the IEEE/CVF international conference on computer vision*, pages 15283–15292, 2021. 2

[3] Martin Hahner, Christos Sakaridis, Mario Bijelic, Felix Heide, Fisher Yu, Dengxin Dai, and Luc Van Gool. Lidar snowfall simulation for robust 3d object detection. In *Proceedings of the IEEE/CVF conference on computer vision and pattern recognition*, pages 16364–16374, 2022.

[4] Velat Kilic, Deepti Hegde, Vishwanath Sindagi, A Brinton Cooper, Mark A Foster, and Vishal M Patel. Lidar light scattering augmentation (lisa): Physics-based simulation of adverse weather conditions for 3d object detection. *arXiv preprint arXiv:2107.07004*, 2021. 2

[5] Xianghao Kong, Wentao Jiang, Jinrang Jia, Yifeng Shi, Runsheng Xu, and Si Liu. Dusa: Decoupled unsupervised sim2real adaptation for vehicle-to-everything collaborative perception. In *Proceedings of the 31st ACM International Conference on Multimedia*, pages 1943–1954, 2023. 2

[6] Yiming Li, Shunli Ren, Pengxiang Wu, Siheng Chen, Chen Feng, and Wenjun Zhang. Learning distilled collaboration graph for multi-agent perception. *Advances in Neural Information Processing Systems*, 34:29541–29552, 2021. 9, 11, 12, 13, 20, 21, 22, 23

[7] Steffen Schneider, Evgenia Rusak, Luisa Eck, Oliver Bringmann, Wieland Brendel, and Matthias Bethge. Improving robustness against common corruptions by covariate shift adaptation. *Advances in neural information processing systems*, 33:11539–11551, 2020. 3

[8] Dequan Wang, Evan Shelhamer, Shaoteng Liu, Bruno Olshausen, and Trevor Darrell. Tent: Fully test-time adaptation by entropy minimization. *arXiv preprint arXiv:2006.10726*, 2020. 3

[9] Tsun-Hsuan Wang, Sivabalan Manivasagam, Ming Liang, Bin Yang, Wenyuan Zeng, and Raquel Urtasun. V2vnet: Vehicle-to-vehicle communication for joint perception and prediction. In *Computer Vision–ECCV 2020: 16th European Conference, Glasgow, UK, August 23–28, 2020, Proceedings, Part II 16*, pages 605–621. Springer, 2020. 9, 11, 12, 13, 16, 17, 18, 19, 20, 21, 22, 23

[10] Runsheng Xu, Zhengzhong Tu, Hao Xiang, Wei Shao, Bolei Zhou, and Jiaqi Ma. Cobevt: Cooperative bird's eye view semantic segmentation with sparse transformers. *arXiv preprint arXiv:2207.02202*, 2022. 3, 9, 11, 12, 13, 14, 16, 17, 18, 19, 20, 21, 22, 23

[11] Runsheng Xu, Hao Xiang, Zhengzhong Tu, Xin Xia, Ming-Hsuan Yang, and Jiaqi Ma. V2x-vit: Vehicle-to-everything cooperative perception with vision transformer. In *European conference on computer vision*, pages 107–124. Springer, 2022. 9, 11, 12, 13, 16, 17, 18, 19, 20, 21, 22

[12] Runsheng Xu, Hao Xiang, Xin Xia, Xu Han, Jinlong Li, and Jiaqi Ma. Opv2v: An open benchmark dataset and fusion pipeline for perception with vehicle-to-vehicle communication. In *2022 International Conference on Robotics and Automation (ICRA)*, pages 2583–2589. IEEE, 2022. 2, 3, 9, 11, 12, 13, 15, 16, 17, 18, 19, 20, 21, 22, 23

[13] Kaiyang Zhou, Yongxin Yang, Yu Qiao, and Tao Xiang. Domain generalization with mixstyle. In *International Conference on Learning Representations (ICLR)*, 2021. 3

[14] Kaiyang Zhou, Yongxin Yang, Yu Qiao, and Tao Xiang. Mixstyle neural networks for domain generalization and adaptation. *International Journal of Computer Vision*, 132 (3):822–836, 2024. 3